INTEGRAL EQUATION METHODS FOR EIGENVALUE ESTIMATION IN SYSTEMS WITH DISCONTINUOUS COEFFICIENTS

By

John Patrick Spence

A DISSERTATION

Submitted to
Michigan State University
in partial fulfillment of the requirements
for the degree of

DOCTOR OF PHILOSOPHY

Department of Mechanical Engineering

1981

ABSTRACT

INTEGRAL EQUATION METHODS FOR EIGENVALUE ESTIMATION
IN SYSTEMS WITH DISCONTINUOUS COEFFICIENTS

By

John Patrick Spence

Systems with abruptly varying physical properties occur in many contexts, both natural and artificial. Of particular interest is the solution of eigenvalue problems which arise in the mathematical models of composite systems. The analysis of such problems hinges on the development of effective and appropriate approximate methods, since exact solution of eigenvalue equations is only possible in the simplest of discontinuous systems. It has been found that traditional techniques which are quite effective in determining the dynamic characteristics of systems with slowly varying properties do not perform nearly as well in discontinuous systems without the application of considerable extra effort.

In the present work, the advantages of taking an integral equation approach to problems in eigenvalue estimation in discontinuous systems are investigated. The inherent smoothing properties of integrals suggest that methods based on integral equations should be quite effective in handling systems with discontinuous material properties.

It is found that the integral equation formulation of the Galerkin method leads to upper bounds for the eigenvalues which are superior to

those obtained from the traditional differential equation formulation. Furthermore, the usually unavailable lower bounds to the eigenvalues may be readily computed by the use of trace identities involving the kernel of the integral equation and infinite sums of powers of the eigenvalues. These lower bounds complement any set of upper bounds and, by their convergence behavior, give insight into the distribution of the generally irregular spectra of discontinuous systems.

ACKNOWLEDGEMENTS

I wish to express my appreciation to the many people who have inspired, encouraged and supported me during the course of my research.

First, I wish to thank my major advisor, Dr. Albert N. Andry, Jr., for convincing me to persevere in the doctoral program and for being an excellent sounding board for my ideas.

I also wish to thank Dr. Cornelius O. Horgan for bringing the problem addressed in this dissertation to my attention and for his continuing guidance and encouragement in bringing this work to fruition.

I also appreciate the contribution of the other members of my guidance committee, Drs. David Yen and James Beck; for their careful reading and suggestions in clarifying the mathematical statement and areas of application of the methods used in this work.

I am also grateful to all my instructors for the knowledge and intuition imparted to me during the course of my degree program and to Ms. Judy Duncan for her timely and accurate typing of this dissertation.

But most of all, I wish to thank my wife, Jan, for her loving support and patience, without which this work would never have come to pass.

TABLE OF CONTENTS

TABLE OF CONTENTS (continued)

LIST OF TABLES

LIST OF FIGURES

INTRODUCTION

Systems with abrupt changes in physical properties occur in many contexts in nature and engineering. Among the naturally occurring systems are the layered structure of skin and teeth, the lipid bilayer biological membranes which separate regions of differing solute concentrations, and rock layers in the earth. Problems of engineering interest include vibration and buckling of stepped shafts, wave propagation through composite media, cooling of nuclear fuel rods and redistribution of impurities in semiconductors.

Exact solution of the eigenvalue problems posed in the mathematical models of discontinuous systems such as these are only possible in the simplest of cases. Thus the analysis of such systems depends on the development of appropriate approximate methods. It has been found that traditional techniques which are quite effective in determining the eigenvalues of systems with slowly varying properties do not perform nearly as well in these discontinuous systems, unless considerable additional effort is applied. Further, accurate lower bounds to the eigenvalues are generally unavailable from these methods.

In this dissertation, a series of eigenvalue problems arising from the application of the technique of separation of variables to linear partial differential equations with linear time invariant boundary conditions are analyzed. These problems are all essentially one dimensional, but the methods used are not restricted to cases which

are or can be made to be such. As shall be seen in the following chapters, the crux of the integral equation formulations prerequisite to applying the methods of this dissertation lies in the availability or derivability of a static impulse response or Green's function. In one-dimensional cases over a finite region, the Green's functions may be found in a closed form which makes the eigenvalue problems in their integral equation form tractable by formally exact methods. However, in problems which cannot be reduced to one spatial dimension by techniques such as conformal mapping or separation of variables, the Green's function itself must be approximated. This, although by no means a trivial task, may be accomplished by methods such as finite differences or finite elements to any desired degree of accuracy. Once a suitably accurate impulse response has been determined, the methods of this dissertation may be applied to find eigenvalue estimates for the new model defined by the Green's function approximation.

Past work in the area of eigenvalue estimation includes use of Laplace transform methods [1,2] finite difference methods [3-5], Sturm-Liouville theory [6-9,12] and many variational schemes. Among the variational approaches taken are Rayleigh-Ritz schemes using both smooth, non-smooth and piecewise defined test functions [6,7,10-17,19] and saddle point variational principles [12-16,19]. Lower bounds for eigenvalues have been obtained by Weinstein's method of intermediate problems [18] and application of results from Sturm-Liouville theory [6,7,12] and eigenvalue extremization [7,19,20]. Some of the lower bound results based on integral equation techniques from the third chapter of this dissertation also appear in [20]. More detailed

expositions of the advantages and pitfalls of these methods are in the application chapters of this dissertation.

In the present work, the advantages of taking an integral equation approach to problems in eigenvalue estimation are investigated. The inherent smoothing properties of integrals suggest that methods based on integral equations should be quite effective in handling systems with discontinuous material properties. For example integral equation methods have proven quite effective in a problem of beam vibration with random coefficients [21]. Variational methods, such as the Rayleigh-Ritz or Galerkin methods, developed in the context of differential formulations of the problems, may also be applied to the integral equation formulation to obtain upper bounds for the eigenvalues. Additionally, lower bounds to complement the upper bounds from variational methods may be readily computed, a distinct advantage over the differential formulations. The lower bounds in each case are presented in terms of basic parameters of the system in question and thus allow a parametric analysis of the dependence of the eigenvalues on system characteristics.

In Chapters 1 and 2 of this dissertation, the fundamental concepts of integral equation theory and some of the results applicable to eigenvalue estimation are discussed. Chapter 3 presents the results of applying both upper and lower bound integral equation methods to heat conduction in a layered slab, comparing the results to those obtained by eigenvalue extremization and differential equation variational methods. In Chapter 4, lower bounds are computed for the frequencies

of vibration of stepped beams, and are compared to those from the method of intermediate problems. Chapter 5 addresses a problem of wave propagation, where lower bounds are found for the frequencies of non-dispersive wave forms travelling normal to the interfaces of laminated composites. In Chapter 6, upper and lower bounds are found by integral equation methods for the frequencies of vibration of a circular membrane with a stepped radial density. The results of this study, together with some suggestions for further study, are summarized in Chapter 7.

The results of this study indicate that integral equation methods may be profitably employed in the analysis of the dynamics of composite structures.

CHAPTER 1

FUNDAMENTALS OF INTEGRAL EQUATIONS

This chapter presents the basic definitions and theorems of the theory of linear integral equations used in the subsequent chapters of this dissertation. The particulars of the integral equation based techniques used to bound eigenvalues are presented in Chapter 2. For a more detailed exposition of the theory of integral equations, see the books of Cochran [22], Tricomi [23] and Stakgold [24].

1.1 Basic Concepts of Linear Integral Equation Theory

Generally speaking, any equation which incorporates an unknown function under one or more signs of integration is an integral equation. Foregoing technical assumptions concerning smoothness, two particular classes of interest are the Fredholm integral equations of the first kind

$$\psi(x) = \int_a^b k(x,y)\phi(y)dy \tag{1.1}$$

and of the second kind

$$\phi(x) = \psi(x) + \lambda \int_a^b k(x,y)\phi(y)dy \tag{1.2}$$

In these equations, ϕ is the unknown function, λ is a complex parameter, and ψ and k are known functions. The function k(x,y) is called the kernel of the integral equation. Notationally, the independent variables are suppressed and the integral is written as

$$K\phi \equiv \int_a^b k(x,y)\phi(y)dy.$$

Thus the Fredholm integral equations in operator form are written as

$$K\phi = \psi$$

and (1.3)

$$\phi = \psi + \lambda K\phi.$$

This operator notation is reminiscent of that found in linear algebra; in fact, much of the terminology and theory are analogous. Matrix algebra is easily imbedded in linear integral equation theory, since summation over a discrete index may be considered as integration of step functions over a continuous index. Thus the definitions and theorems that follow may be viewed as generalizations of the familiar notions of linear algebra.

Definition 1.1 The complex valued functions $f(x)$ and $k(x,y)$ are said to be square-integrable or L^2 if the quantities

$$||f|| \equiv \{\int_a^b |f(x)|^2 dx\}^{1/2}$$

and

$$||K|| \equiv \{\int_a^b \int_a^b |k(x,y)|^2 dydx\}^{1/2}$$

are finite. The dependence on the domain of integration is sometimes denoted by saying that f is $L^2(a,b)$.

Definition 1.2 For $f, g \in L^2(a,b)$ the complex inner product of f and g is defined by

$$\langle f,g\rangle \equiv \int_a^b f(x)\overline{g}(x)dx$$

where the superior bar denotes complex conjugation.

Definition 1.3 Two $L^2(a,b)$ functions f and g are said to be orthogonal if $\langle f,g\rangle = 0$.

Theorem 1.1 The complex inner product $\langle \cdot,\cdot \rangle$ satisfies the following properties for f, g, $h \in L^2(a,b)$ and α, β complex scalars:

(1) $\langle \alpha f + \beta g,h\rangle = \alpha\langle f,h\rangle + \beta\langle g,h\rangle$

(2) $\langle g,f\rangle = \overline{\langle f,g\rangle}$

(3) $\langle f,f\rangle \geq 0$ with equality if and only if $f = 0$ (almost everywhere).

Theorem 1.2 Let f and g be elements of $L^2(a,b)$. Then the functional $||\cdot||$ is an inner product norm; that is

(1) $||\lambda f|| = |\lambda|\ ||f||$ where λ is a complex scalar

(2) $||f+g|| \leq ||f|| + ||g||$ (Minkowski inequality)

(3) $||f|| \geq 0$ with equality if and only if $f = 0$ (almost everywhere).

Further, the inner products $\langle \cdot, \cdot \rangle$ and norm $||\cdot||$ satsify

(4) $|\langle f,g\rangle| \leq ||f||\cdot||g||$ (Schwartz inequality)

Theorem 1.3 $L^2(a,b)$, under the inner product norm $||\cdot||$, contains the limits of all Cauchy sequences of elements of $L^2(a,b)$. Thus $L^2(a,b)$ is a Hilbert space (complete normed linear vector space with inner product norm).

Definition 1.4 The adjoint $k^*(x,y)$ of the kernel $k(x,y)$ is given by the complex conjugate of the transpose of k; that is

$$k^*(x,y) = \overline{k}(y,x),$$

and, in operator notation, the adjoint K^* of K is defined by

$$K^*\phi \equiv \int_a^b k^*(x,y)\phi(y)dy.$$

Remark: An alternative definition based on the L^2 inner product is that K^* is the operator with kernel k^* satisfying, for all $f, g \in L^2(a,b)$,

$$\langle Kf,g\rangle = \langle f,K^*g\rangle$$

Definition 1.5 The trace of the operator K with L^2 kernel $k(x,y)$ is given by

$$tr(K) \equiv \int_a^b k(x,x)dx$$

Definition 1.6 The composition k of two kernels k_1 and k_2 is given by

$$k(x,y) = \int_a^b k_1(x,z)k_2(z,y)dz$$

and one writes in operator notation

$$K = K_1K_2.$$

Theorem 1.4 Let K_1 and K_2 be linear integral operators with L^2 kernels k_1 and k_2. Then the composite kernel of $K \equiv K_1K_2$ is L^2, and

$$(1) \quad ||K|| = ||K_1K_2|| \leq ||K_1|| \cdot ||K_2||$$

Further, if ϕ is $L^2(a,b)$ so is $\psi = K\phi$ with

(2) $||\psi|| \leq ||K|| \cdot ||\phi||$

Definition 1.7 A kernel $k(x,y)$ (or operator K) is said to be Hermitian if $k = k^*$ (or $K = K^*$). If k is real valued and Hermitian, it is said to be symmetric. If $KK^* = K^*K$, K is said to be normal; all Hermitian kernels have this property.

Definition 1.8 A Fredholm integral equation of the second kind, $\phi = \psi + \lambda K\phi$, is said to be homogeneous if $\psi = 0$.

Definition 1.9 A value of the complex parameter λ in the homogeneous equation $\phi = \lambda K\phi$ which admits only the trivial solution $\phi \equiv 0$ is called a regular value of K. Values of λ admitting a nontrivial solution $\phi \not\equiv 0$ are called eigenvalues of K, and ϕ is an eigenfunction of K belonging to λ.

Theorem 1.5 Let K be a linear integral operator with L^2 kernel $k(x,y)$. Then:

(1) The eigenvalues of a Hermitian kernel form a non-void finite or countable sequence $\{\lambda_n\}$ of real numbers ordered by their magnitude $0 < |\lambda_1| \leq |\lambda_2| \leq \ldots$; this sequence has no finite limit point.

(2) The eigenfunctions of the Hermitian kernel k belonging to distinct eigenvalues are orthogonal and may be chosen to have norm 1; that is, they can be chosen orthonormal.

(3) The eigenfunctions of a symmetric kernel k may be chosen to be real.

(4) The finite number of eigenfunctions belonging to any distinct eigenvalue λ of a Hermitian kernel k may be chosen to be orthonormal.

(5) If $\phi_1, \phi_2, \ldots \phi_N$ are distinct orthonormal eigenfunctions of a Hermitian kernel k belonging to the eigenvalues $\lambda_1, \lambda_2, \ldots \lambda_N$ (not necessarily distinct), then Bessel's inequality holds:

$$\sum_{i=1}^{N} \frac{|\phi_i(x)|^2}{\lambda_i^2} \leq \int_a^b |K(x,y)|^2 dy$$

(6) Integration of the inequality (5) leads to

$$\sum_{i=1}^{N} (\lambda_i)^{-2} \leq ||K||^2$$

and if each eigenvalue of K, repeated according to its multiplicity, is included in the sum, equality holds.

1.2 Formulation of Integral Equation Eigenvalue Problems

One way of obtaining linear integral equation eigenvalue problems is to transform linear differential eigenvalue problems to integral form. This is accomplished by using an associated Green's function which captures both the internal and boundary behavior of the underlying differential equation in terms of the response to unit point excitation [25]. For example, examine the following linear differential eigenvalue problem:

$$\begin{aligned} L[u] &= \lambda M[u] \quad \text{on domain } D \\ B[u] &= 0 \qquad \text{on boundary } \partial D. \end{aligned} \tag{1.4}$$

The operators L, M, and B are linear and do not depend on the eigenparameter λ. If one then can solve the associated problem

$$\begin{aligned} L[G(x,y)] &= \delta(x-y) \quad \text{on } D \\ B[G(x,y)] &= 0 \qquad \text{on } \partial D, \end{aligned}$$

where L and B are understood to operate on the x dependence of $G(x,y)$ and δ is the Dirac delta distribution, the solution to an equation $L[u] = v$, $B[u] = 0$ is given by

$$u(x) = \int_D G(x,y)v(y)dy.$$

In particular then, the eigenvalue problem 1.4 can be expressed as

$$u(x) = \lambda \int_D G(x,y)M[u](y)dy \tag{1.5}$$

In the case where L and B lead to a self-adjoint problem, that is, if for all functions u and v (for which the equation makes sense),

$$\langle u, L[v] \rangle = \langle L[u], v \rangle,$$

the resulting Green's function is Hermitian. However the integral equation 1.5 does not have a Hermitian kernel unless $M[u](y) = m \cdot u(y)$ for some scalar $m \neq 0$. In the case where M is algebraic, $M[u](y) = m(y)u(y)$, with $m(y) > 0$, the equation 1.5 can be made to have a Hermitian kernel by the substitutions

$$\begin{aligned} \phi(\cdot) &= \sqrt{m(\cdot)}\, u(\cdot) \\ k(x,y) &= \sqrt{m(x)}G(x,y)\sqrt{m(y)} \end{aligned} \tag{1.6}$$

giving the eigenvalue problem with Hermitian kernel k,

$$\phi(x) = \lambda \int_D k(x,y)\phi(y)dy$$

or (1.7)

$$\phi = \lambda K \phi.$$

CHAPTER 2

INTEGRAL EQUATION EIGENVALUE ESTIMATION PROCEDURES

This chapter outlines the basis and mechanics of the procedures used in this dissertation to provide upper and lower bounds for the eigenvalues in the examples of the subsequent chapters. Upper bounds to the eigenvalues are obtained by the Galerkin method, which for Hermitian kernels coincides with the traditional Rayleigh-Ritz method. Lower bounds are computed using these upper bounds and the trace of a related kernel. For a more detailed exposition of these methods and many others, see the excellent book of Baker [26].

2.1 The Galerkin Method

The essence of the Galerkin method is the use of finite expansions of the true eigenfunctions in a series of appropriately chosen known functions. That is, a true eigenfunction ψ of the eigenvalue problem $\psi - \lambda K\psi = 0$ is approximated by

$$\hat{\psi} \equiv \Sigma a_j \phi_j \tag{2.1}$$

where the a_j are as yet undetermined constants and the ϕ_j are linearly independent functions. If the approximant is substituted into the expression $\psi - \lambda K\psi$ one obtains an error term $r(x)$,

$$\hat{\psi} - \lambda K\hat{\psi} = r(x). \tag{2.2}$$

Various minimizations of the error term lead to the expansion approximation methods. In the general Galerkin method, the constants a_j and λ are found by requiring that the error term be orthogonal to the test functions used under a weighted inner product with known positive L^2 weight $w(x)$ defined by

$$\langle f,g\rangle_w \equiv \int_a^b f(x)\overline{g}(x)w(x)dx.$$

One possible choice of w is $w(x) \equiv 1$, leading to orthogonality under the usual L^2 inner product.

If Equation 2.2 is multiplied by $\overline{\phi}_i$ and integrated over the domain, one obtains

$$\sum_j a_j\langle\phi_j,\phi_i\rangle - \lambda \sum_j a_j\langle K\phi_j,\phi_i\rangle = \langle r,\phi_i\rangle$$

for each $i = 1, 2, \ldots n$. If the matrices A and B are defined by

$$\begin{aligned} A_{ij} &\equiv \langle\phi_j,\phi_i\rangle \\ B_{ij} &\equiv \langle K\phi_j,\phi_i\rangle \end{aligned} \tag{2.3}$$

requiring that the error term be orthogonal to the test functions used leads to the general matrix eigenvalue problem for the a_i and λ

$$(A - \hat{\lambda}B)\hat{a} = 0. \tag{2.4}$$

The choice of linearly independent test functions guarantees that A is nonsingular. Further, it is clear that A is Hermitian, since by Theorem 1.1,

$$\langle\phi_j,\phi_i\rangle = \langle\overline{\phi_i,\phi_j}\rangle.$$

If the kernel $k(x,y)$ is Hermitian, the matrix B is as well, since

$$\begin{aligned} \langle K\phi_j,\phi_i\rangle &= \langle \phi_j, K^*\phi_i\rangle && \text{(Definition 1.4)} \\ &= \langle \phi_j, K\phi_i\rangle && \text{(Definition 1.7)} \\ &= \overline{\langle K\phi_i,\phi_j\rangle}. && \text{(Theorem 1.1)} \end{aligned}$$

That the approximate eigenvalues obtained by the Galerkin procedures are upper bounds in magnitude to the actual eigenvalues is a consequence of the Poincare characterization of the eigenvalues, namely

$$\frac{1}{\lambda_n} = \max_{S^{(n)}} \min_{\phi\varepsilon S^{(n)}} \langle K\phi,\phi\rangle/\langle\phi,\phi\rangle$$

where $S^{(n)}$ ranges over all n-dimensional subspaces of L^2. This result is stated in the following theorem proven in Baker [26], page 321.

Theorem 2.1 Let $k(x,y)$ be a Hermitian L^2 kernel, $\phi_1, \ldots \phi_n$ linearly independent L^2 functions, and A and B the Galerkin matrices from Equations 2.3a and 2.3b . Then if $\hat{\lambda}_r^+(\hat{\lambda}_r^-)$ is the rth positive (negative) eigenvalue satisfying $(A - \hat{\lambda}B)\hat{a} = 0$, then

$$\lambda_r^+ \leq \hat{\lambda}_r^+ \qquad (\lambda_r^- \geq \hat{\lambda}_r^-)$$

provided λ_r^-, $\hat{\lambda}_r^+(\lambda_r^-,\hat{\lambda}_r^-)$ both exist.

A choice of a complete sequence of test functions leads to the monotone convergence of the approximate eigenvalues to the actual and thus completeness in L^2 is a desirable property for the test functions chosen to have. Further characteristics of the test functions leading to generally better results are that they share as many of the known properties of the true eigenfunctions as possible, such as boundary

conditions, number of zeros in the interval, and, of some consequence in discontinuous systems, smoothness conditions at internal points.

It should be noted that the convergence of the approximate eigenfunctions as more terms are added is in a mean-square sense to the actual eigenfunctions. In cases where there are jumps in the actual eigenfunctions (or their derivatives), the use of continuous (or smooth) test functions can lead to poor uniform approximations. These effects are ameliorated by the use of $K\phi_j$ rather than the ϕ_j in the eigenfunction approximations; the iterated Galerkin method [27].

2.2 Lower Bounds by Trace Identities

Define the iterated kernels $k^{(n)}(x,y)$ by the recursion

$$\begin{aligned} k^{(1)}(x,y) &\equiv k(x,y) \\ k^{(n+1)}(x,y) &\equiv \int_a^b k(x,z)k^{(n)}(z,y)dz. \end{aligned} \tag{2.5}$$

Then if k is L^2 so are each of the $k^{(n)}$. Further, the following theorem holds:

Theorem 2.2 ([22], pg. 51) Let k(x,y) be an L^2 kernel with spectrum $0 < |\lambda_1| \leq |\lambda_2| \leq \ldots$. Then for $n \geq 2$,

$$tr(K^{(n)}) = \int_a^b k^{(n)}(x,x)dx = \sum_{i=1}^{\infty} \lambda_i^{-n}.$$

Of particular interest is the case when k is Hermitian and positive definite. In this case truncation of the series leads to

$$tr(K^{(n)}) = \sum_{i=1}^{\infty} \lambda_i^{-n} \geq \lambda_j^{-n}, \quad j = 1, 2, \ldots$$

giving the lower bound

$$\lambda_j \geq (\mathrm{tr}(K^{(n)}))^{-1/n}. \tag{2.6}$$

This bound is of course most accurate for the least eigenvalue.

If a set of M upper bounds $\overline{\lambda}_i$ is available, then the inequality (2.6) may be improved considerably:

$$\mathrm{tr}(K^{(n)}) = \sum_{i=1}^{\infty} \lambda_i^{-n}$$

$$\geq \lambda_m^{-n} + \sum_{i \neq m}^{M} \lambda_i^{-n}$$

$$\geq \lambda_m^{-n} + \sum_{i \neq m}^{M} \overline{\lambda}_i^{-n}$$

giving the lower bounds

$$\lambda_m \geq (\mathrm{tr}(K^{(n)}) - \sum_{i \neq m}^{M} \overline{\lambda}_i^{-n})^{-1/n} \tag{2.7}$$

This bound differs from each m, and is improvable by obtaining either more or better upper bounds.

In this dissertation, the bounds obtained from the particular case of n=2 are used and are denoted by

$$\underline{\lambda}_1^{(0)} \equiv (\mathrm{tr}(K^{(2)}))^{-1/2} \tag{2.8}$$

and

$$\underline{\lambda}_m^{(M)} \equiv (\mathrm{tr}(K^{(2)}) - \sum_{i \neq m}^{M} \overline{\lambda}_i^{-2})^{-1/2}, \tag{2.9}$$

and are called the truncation lower bound and the corrected truncation lower bound respectively.

CHAPTER 3

STURM-LIOUVILLE PROBLEMS WITH DISCONTINUOUS COEFFICIENTS

3.1 Introduction and Literature Review

This chapter addresses the problem of eigenvalue estimation for Sturm-Liouville problems with discontinuous coefficients in the context of diffusion in a laminated medium. Other problems of the Sturm-Liouville form that have been the subject of much recent attention include vibration problems in geophysics [8,9,28], buckling of stepped beams [12,18], and harmonic waves in layered composites [6,10-15,19], among others. The latter problem is discussed in Chapter 5 of this dissertation.

Considerable emphasis has been placed on the development of computational schemes for estimating the eigenvalues and eigenfunctions for such problems. These efforts have met with serious difficulties due to the non-smoothness of the coefficients and the resulting spectral irregularities. Early attempts were focused mainly on variational techniques, with emphasis on obtaining upper bounds for the eigenvalues. These techniques include Rayleigh-Ritz approximation using smooth test functions and improved test functions with appropriate derivative discontinuities [7,12,19]. Also in the variational mode, mixed variational principles where two field quantities are independently varied have been employed [7,12,19]. Alternative methods, such as finite difference

and finite element methods, which lead to matrix eigenvalue problems, have been investigated [3-5]. A direct variational scheme employing piecewise polynomial eigenfunction approximation has also been used [17]. More recently, results from classical Sturm-Liouville theory and eigenvalue optimization techniques have been adapted for these problems to obtain upper and lower bounds for the eigenvalues [7,12,19]. The most valuable contribution of [7] was the reduction of the general Sturm-Liouville problem to that of a string with discontinuous density. In this simpler form, the various techniques are more easily applied and give better results for a comparable amount of effort. Lower bounds have also been found by a variation on Weinstein's method of intermediate problems [18]. A complete theoretical discussion of diffusion in laminated media under general linear interface conditions has been set forth in [29], with an extensive bibliography.

In this chapter, integral equation methods are applied to a problem of heat conduction in a layered slab with fixed temperature boundary conditions and perfect thermal contact interface conditions. Lower bounds to the least eigenvalue obtained using the iterated kernel trace are compared to those based on eigenvalue extremization discussed in [19]. Upper bounds are generated using Galerkin's method applied to both the differential and integral equation formulations of the problem. These upper bounds are compared in terms of their accuracy and are also used to generate the sequences of lower bounds for higher eigenvalues obtained by correction of the truncation of the series summing to the iterated kernel trace. The actual eigenvalues, obtained by numerical solution of the actual transcendental eigenvalue equation, are used

to compute errors in the bounds. Numerical results are presented for a variety of material property combinations, and sources of error in the approximate methods are discussed. The results suggest that integral equation techniques, with their inherent smoothing properties, may be particularly appropriate for investigation of the problems of concern here.

3.2 Eigenvalue Problem Formulation

The general partial differential equation modelling diffusion with no internal sources is

$$\nabla\cdot(\kappa\nabla u) = c\,\frac{\partial u}{\partial t}. \tag{3.1}$$

In the one-dimensional problem of heat conduction in a layered slab with fixed surface temperature and perfect thermal contact between the layers, separation of spatial and temporal variables leads to the Sturm-Liouville problem:

$$\begin{aligned} &(\kappa(x)u'(x))' + \lambda\, c(x)u(x) = 0 \qquad && 0 \le x \le L \\ &\quad u(0) = u(L) = 0 \qquad && \\ &u(x),\ \kappa(x)u'(x) \text{ continuous for } 0 < x < L \qquad && \end{aligned} \tag{3.2}$$

The coefficient functions κ and c, representing conductivity and capacity respectively, are piecewise continuous positive functions with step discontinuities at the interface locations $x_1, x_2, \ldots x_n$.

It has been recently demonstrated [7] that conversion of the problem (3.2) to Liouville normal form leads to computational advantages. Thus, let

$$T = \int_0^L \kappa^{-1}(s)ds, \quad t = T^{-1} \int_0^x \kappa^{-1}(s)ds$$

and (3.3)

$$v(t) = u(x(t)), \qquad f(t) = T^2\kappa(x(t))c(x(t)).$$

Then the eigenvalues of the system (3.2) are the same as those of

$$\begin{aligned} &\ddot{v} + \lambda f v = 0 \qquad 0 \leq t \leq 1 \\ &v(0) = v(1) = 0 \\ &v, \dot{v} \text{ continuous for } 0 < t < 1 \end{aligned} \tag{3.4}$$

where the superposed dot represents differentiation with respect to the new independent variable t. The coefficient function f(t) is positive and bounded for $0 \leq t \leq 1$ and admits step discontinuities at the points $t_i = T^{-1} \int_0^{x_i} \kappa^{-1}(s)ds$. The effect of the transformation has been to remove the discontinuous coefficient κ from its position subject to differentiation in the system (3.2) and move the locations of the discontinuities. When standard variational methods using smooth test functions are applied to the transformed system (3.4), the results are equivalent to those obtained using improved test functions satisfying the condition of continuity in flux, $\kappa u'$, with less computational effort. A further advantage of this form is the availability of lower bounds to the eigenvalues based on eigenvalue extremization in vibrating strings.

3.3 Integral Equation Formulation

The eigenvalue problem (3.4) is readily transformed to the integral equation

$$v(t) = \lambda \int_0^1 G(t,s)f(s)v(s)ds \tag{3.8}$$

where

$$G(t,s) = \begin{cases} (1-s)t & 0 \leq t \leq s \leq 1 \\ (1-t)s & 0 \leq s \leq t \leq 1 \end{cases} \tag{3.9}$$

is the Green's function, obtained by solving

$$-\frac{\partial^2 G}{\partial t^2}(t,s) = \delta(t-s);\ G(0,s) = G(1,s) = 0. \tag{3.10}$$

Note that if we view the kernel of the integral equation as

$$\hat{k}(t,s) = G(t,s)f(s) \tag{3.11}$$

then the kernel is not symmetric in s and t. However, we may obtain an integral equation with symmetric kernel by multiplying (3.8) by $\sqrt{f(t)}$ and thus obtaining the equivalent eigenvalue problem

$$\psi(t) = \lambda \int_0^1 k(t,s)\psi(s)ds = \lambda K\psi \tag{3.12}$$

where $\psi(t) = \sqrt{f(t)}\ v(t)$ and $k(t,s) = \sqrt{f(t)}\ G(t,s)\ \sqrt{f(s)}$. Equation (3.12) is a Fredholm integral equation of the second kind with a kernel which, although discontinuous in s and t, is real, symmetric, square-integrable and continuous in the mean [30]. The trace of the second iterate of this kernel, which equals the L^2 norm of the kernel, is given by the double integral

$$\mathrm{tr}(K^{(2)}) = \int_0^1 \int_0^1 f(t)G^2(t,s)f(s)dsdt \tag{3.13}$$

In the case of piecewise constant f(t), this equation involves easy integrations of polynomials of degree ≤ 3 in s and t over appropriate subregions of the unit square, and are easily carried out either by hand or numerically.

3.4 Lower Bounds by Eigenvalue Extremization

Lower bounds for the eigenvalues of (3.2) have been obtained in [19] based on the normal form (3.4) and the results of Krein [31] on eigenvalue extremization. In [31], Krein is concerned with the problem of maximizing and minimizing the eigenfrequencies $\omega_n^2(f)$ of a string of variable density f, as in (3.4), subject to the constraints on f of a fixed total mass

$$\int_0^1 f(t)dt = M \tag{3.14}$$

and various bounds on the density, such as

$$\begin{aligned} &0 < f \leq H \quad \text{with} \quad H \geq M \\ &0 < h \leq f \quad \text{with} \quad h \leq M \end{aligned} \tag{3.15}$$

Under conditions (3.14), (3.15b) the minimum λ_1 is attained by the singular function

$$f(t) = h + (M-h)\delta(t-1/2) \tag{3.16}$$

which may be viewed as a uniform string with a bead at the center. Under the conditions (3.14), (3.15a) the minimum λ_1 is attained by

$$f(t) = \begin{cases} H & |2t - 1| < M/H \\ 0 & \text{otherwise.} \end{cases} \tag{3.17}$$

The maximizing densities for the higher eigenvalues λ_n have n equally spaced beads or dense intervals at the antinodal points of the nth eigenfunction of a uniform string. Thus we see that Krein's work leads to consideration of problems directly related to the investigation of eigenvalue problems with discontinuous coefficients. This relationship was exploited in [19] and their development follows.

Under the conditions (3.14), (3.15a), Krein [31] has shown that

$$\lambda_n(f) \geq \frac{4n^2H}{M^2}\ \chi\left(\frac{M}{H}\right) \tag{3.18}$$

and under (3.14), (3.15b)

$$\lambda_n(f) \geq \frac{4n^2}{h}\ \chi\left(\frac{h}{M}\right) \tag{3.19}$$

where $\chi(d)$ is the least positive root of the transcendental equation

$$\sqrt{\chi}\ \tan\sqrt{\chi} = d/(1-d) \tag{3.20}$$

The lower bounds may be made explicit on obtaining bounds for the lowest root. One such bound, obtained by Krein [31], is

$$\chi(d) > d\left[1 - \frac{4d}{3} + \left(\frac{11}{24} + \frac{4}{\pi^4}\right)d^2\right]^{-1/2} \tag{3.21}$$

This result, in conjunction with (3.18), was utilized in [19] for n = 1. When used with (3.19) more bounds are found; these results are presented in the next two sections on the example problem.

3.5 Example Problem

In order to evaluate the various bounding techniques, we consider the example of a three layer slab composed of two identical homogeneous outer layers enclosing an inner homogeneous layer as has been treated in [7,12,19]. The piecewise constant material property coefficients κ and c are given by

$$\begin{aligned} &\kappa_1,\ c_1 \text{ in} \quad 1 \geq |2x-1| > b \quad \text{(outer layers)} \\ &\kappa_2,\ c_2 \text{ in} \quad |2x-1| \leq b \quad \text{(inner layer)} \end{aligned} \tag{3.22}$$

The problem is then nondimensionalized and parametrized by the substitutions

$$\gamma = \frac{\kappa_2}{\kappa_1}\ ,\ \theta = \frac{c_2}{c_1}\ ,\quad n_1 = 1-b,\quad n_2 = b, \tag{3.23}$$

$$\bar{\kappa} = n_1\kappa_1 + n_2\kappa_2,\quad \bar{c} = n_1c_1 + n_2c_2,$$

and so, using the normalization $\bar{\kappa} = 1$, $\bar{c} = 1$, we obtain

$$\begin{aligned} c_1 &= (n_1 + n_2\theta)^{-1},\quad c_2 = \theta(n_1+n_2\theta)^{-1} \\ \kappa_1 &= (n_1 + n_2\gamma)^{-1},\quad \kappa_2 = \gamma(n_1 + n_2\gamma)^{-1}. \end{aligned} \tag{3.24}$$

The corresponding dimensionless eigenvalue is then denoted by ν and given by

$$\nu = (\lambda\bar{c}/\bar{\kappa})^{1/2} = \lambda^{1/2}. \tag{3.25}$$

For given values of the geometric parameters n_1 and n_2, the effect of the material discontinuities on ν is conveniently analyzed through consideration of the dependence of ν on the dimensionless material

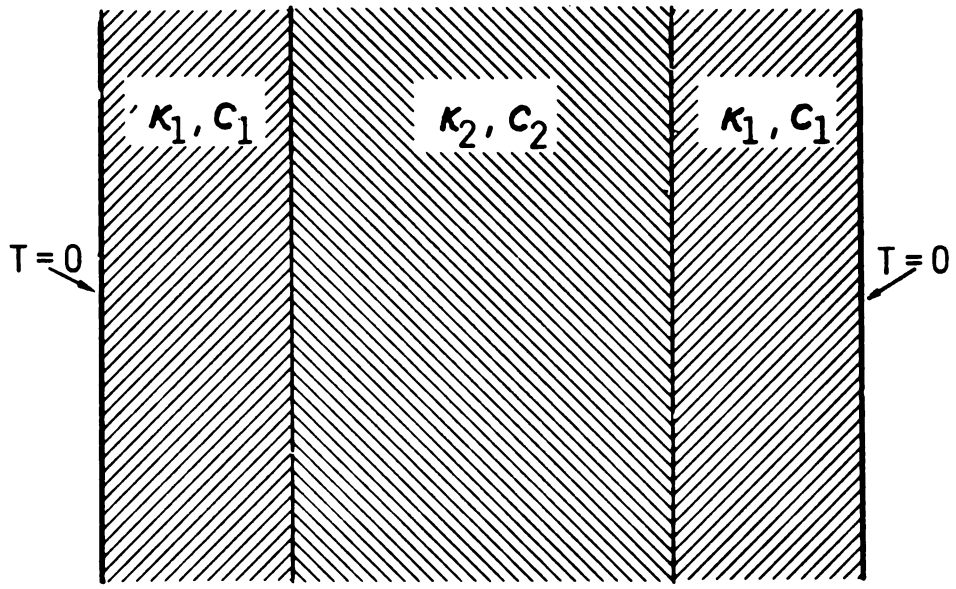

FIGURE 3.1 Layered slab with piecewise constant properties

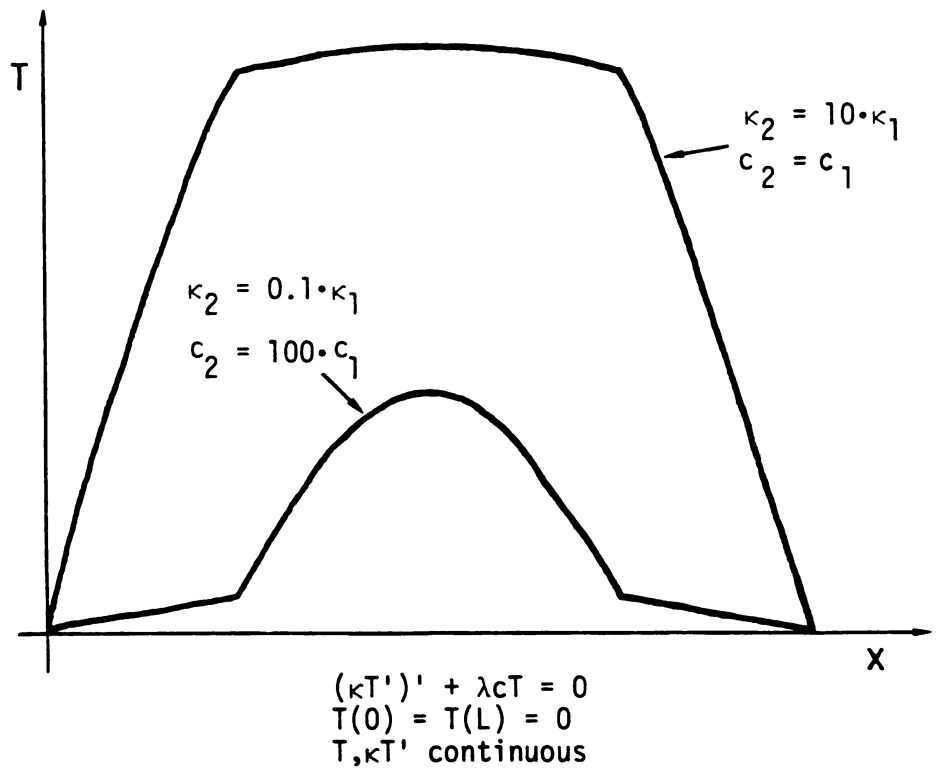

FIGURE 3.2 Fundamental mode temperature profiles

parameters γ and θ. For continuous conductivities $\gamma = 1$, while for continuous capacities $\theta = 1$. Henceforth, we will set $b = 1/2$, giving $n_1 = n_2 = 1/2$ and interfaces at $x_1 = 1/4$ and $x_2 = 3/4$. For this case, the exact eigenvalue equations, obtained by solving (3.2) exactly in each material subinterval and matching temperature and flux at the interfaces, are:

$$\begin{aligned} \sqrt{\lambda\theta}\ \sin\beta\nu\ \sin\alpha\nu - \cos\beta\nu\ \cos\alpha\nu &= 0 \\ \sqrt{\lambda\theta}\ \cos\beta\nu\ \sin\alpha\nu + \sin\beta\nu\ \cos\alpha\nu &= 0 \end{aligned} \tag{3.26}$$

where

$$\alpha = \frac{1}{4}\left(\frac{1+\gamma}{1+\theta}\right)^{1/2}, \qquad \beta = \frac{1}{4}\left(\frac{1+\gamma^{-1}}{1+\theta^{-1}}\right)^{1/2}.$$

The two separate equations for $\nu_1, \nu_3, \ldots$ and $\nu_2, \nu_4, \ldots$ result from the symmetry of the problem about the slab center.

Under this parametrization, the coefficient f(t) in (3.4) is given by

$$f(t) = \begin{cases} h_1 & \left|t - \frac{1}{2}\right| > \frac{1}{2(\gamma+1)} \\ h_2 & \left|t - \frac{1}{2}\right| \leq \frac{1}{2(\gamma+1)} \end{cases} \tag{3.27}$$

where

$$h_1 = \frac{(\gamma+1)^3}{4\gamma^2(1+\theta)}, \qquad h_2 = \gamma\theta h_1.$$

For this f(t), the trace of the second kernel iterate is given by

$$\mathrm{tr}(K^{(2)}) = h_1^2\{\frac{1}{90} - \frac{(\gamma\theta-1)^2}{144}\,\ell(1-\ell)^3(3+\ell^2) +$$

$$\frac{(\gamma\theta)^2-1}{720}\,\ell(15-10\ell^2+3\ell^4)\} \tag{3.28}$$

where $\ell = (1+\gamma)^{-1}$ is the center interval length and $\gamma\theta$ is the coefficient discontinuity ratio in the Liouville normal form.

The truncation lower bound (2.8) for the least eigenparameter ν becomes

$$\nu_1 \geq (\mathrm{tr}(K^{(2)}))^{-1/4}, \tag{3.29}$$

and the lower bounds for higher eigenparameters (2.9) becomes

$$\nu_m \geq (\mathrm{tr}(K^{(2)}) - \sum_{n\neq m} (\overline{\nu}_i)^{-4})^{-1/4} \tag{3.30}$$

An additional parameter to be used in the bounds from Krein [31] is the total "mass"

$$M = \int_0^1 f(t)dt = \frac{(\gamma+1)^2}{4\gamma} \tag{3.31}$$

Thus from (3.18) and (3.19), using (3.20) and the above parametrization, we obtain the lower bounds

$$\nu_n \geq \frac{4n\gamma^{1/2}}{\gamma+1}\,[1 - \frac{4}{3}\,d + (\frac{11}{24} + \frac{4}{\pi^4})\,d^2]^{-1/4} \tag{3.32}$$

where d is given by one of the four expressions:

$$d = \frac{1+\theta^{-1}}{1+\gamma}, \quad \text{if } \gamma\theta \geq 1 \text{ under } f \leq H = h_2,$$

$$d = \frac{1+\gamma^{-1}}{1+\theta}, \text{ if } \gamma\theta \geq 1 \text{ under } f \geq h = h_1,$$

$$d = \frac{1+\theta}{1+\gamma^{-1}}, \text{ if } \gamma\theta \leq 1 \text{ under } f \leq H = h_1,$$

or

$$d = \frac{1+\gamma}{1+\theta^{-1}}, \text{ if } \gamma\theta \leq 1 \text{ under } f \geq h = h_2.$$

3.6 Numerical Results

In order to assess the accuracy and nature of the error involved in the lower bounds based on the iterated kernel trace, a number of bounds were computed for various combinations of material properties. The lower bounds for the least eigenvalue based on truncation of the series at the first term (3.29) are shown in Table 3.1, with the best Krein bound (3.32) and actual eigenvalues from (3.26) for comparison. Upper bound sets from the Galerkin method using trigonometric test functions in the differential and integral formulations are presented for four cases, together with the corresponding lower bound sets from (3.30), in Table 3.2. An additional study of the progressively improving upper and lower bounds obtained as the number of test functions used in the integral Galerkin method increases appears in Tables 3.3 and 3.4. Also in these tables, the best possible lower bounds from (3.30), where the actual eigenvalues are used as the upper bounds, are presented for comparison purposes.

All of the numerical results in this chapter were computed in double precision on the Prime 750 computer of the Case Center for Computer Aided Design at Michigan State University.

3.7 Discussion of Results

Table 3.1 provides a comparison between the integral equation lower bounds (3.29) and the eigenvalue extremization bounds (3.32). In all cases where the Liouville normal form (3.4) has a center weighted density f(t), that is, where the product of the discontinuity ratios, $\gamma\theta$, exceeds or equals one, the extremization bounds (3.32) are quite accurate. When both ratios γ and θ exceed one, the only cases considered in [7,12,19], the integral equation lower bounds (3.29) compare favorably with the extremization bounds (3.32). In mixed cases, where either γ or θ, but not both, and the product $\gamma\theta$ is less than one, the coefficient function f(t) is no longer similar to the extremizing densities (3.16) and (3.17) of Krein, and the corresponding bounds (3.32) are quite poor. In these edge-weighted cases, the accuracy of the integral equation bounds (3.29) suffer as well, but for a quite different reason.

The error induced by using (3.29) depends on the appropriateness of the truncation of the series that sums to the iterated kernel trace, and thus depends on the distribution of the spectrum. The closer the least eigenvalue is to the rest of the spectrum, the less accurate the results of the truncation can be. Table 3.1 shows that the accuracy of (3.29) is exceptional for highly center weighted cases with $\gamma\theta \gg 1$ and falls off for the edge weighted cases with $\gamma\theta < 1$. Using the vibrations of a string as an analogy, one can interpret this phenomenon in terms of the effect of the heavier region on the modes of vibration. In the center weighted cases, the concentration of the mass in the center about the antinodal point of the first mode significantly lowers

the fundamental frequency compared to that obtained for a uniform string. However, this mass concentration occurs about the nodal point of the second mode, and the lesser amplitude of motion reduces the effect on the frequency. Thus the first two frequencies are more widely separated, and the series can be truncated at the first term and still give good results. In contrast, in the edge weighted cases, with $\gamma\theta < 1$, the motion of the concentrated masses near the ends is comparable in the first two modes, and the frequencies are correspondingly closer than those of a uniform string. Such clustering of the lower eigenvalues increases the error due to truncation in (3.29). This defect is remedied by the use of upper bound information as in the bound (3.30), as can be seen in Table 3.2, case 4, where $\gamma = \theta = 0.1$.

In Table 3.2, two sets of six upper bounds and the resulting lower bound sets are presented for four combinations of material properties. Both upper bound sets were obtained using Galerkin's method with test functions of the form

$$v_i(t) = \sum_{j=1}^{6} c_{ij} \sin j\pi t$$

in the differential formulation, and

$$\psi_i(t) = \sqrt{f(t)}\, v_i(t)$$

in the integral formulation. In this particular example problem, the symmetry of the system about the midpoint allows separation into odd and even matrix eigenvalue problems, since the test functions and true eigenfunctions are even and odd about the midpoint, and the

resulting inner products, which constitute the Galerkin matrices, vanish for pairs with different parity.

As can be seen in all four cases in Table 3.2, the upper bounds from the integral equation formulation are superior to those from the differential equation formulation. This leads to a marked superiority of the lower bounds based on the integral formulation. The error in these lower bounds from Equation (3.30) comes from two sources: truncation of the series after six terms and the approximation of the second, or correction, term. The error due to truncation depends on the number of terms used as well as the distribution of the spectrum. The error due to the approximation of the correction term depends primarily on the accuracy of the upper bound for the least eigenvalue used in the correction term.

In Table 3.2, Case 1, the eigenvalues are nearly equally spaced and the upper bounds are quite accurate. In this case, the lower bound error is primarily due to series truncation, the accuracy of the lower bounds increasing only slightly when the better integral equation bounds are used. In Case 2, the spectrum is again nearly equally spaced, but the differential upper bound to ν_1 is significantly less accurate than the integral, leading to far less accurate lower bounds for the rest of the spectrum. This difference is even more pronounced in Cases 3 and 4, but the effects of eigenvalue spacing enter into these bounds as well. Within each case, the accuracies of lower bounds within a cluster of closely spaced eigenvalues are comparable. In Case 3, the lower bounds to the least two isolated eigenvalues are accurate (particularly those from the integral upper bounds), and the lower bounds to the cluster ν_3 - ν_5 are of 27-36

percent relative error, jumping to 53 percent for the isolated ν_6. In Case 4, one cluster is ν_1 - ν_3 and the corresponding lower bounds range from 2-8 percent relative error, ν_4 is isolated with 34 percent relative error, and ν_5 - ν_7 is another cluster with 51-56 percent relative error in the lower bounds.

Tables 3.3 and 3.4 present another examination of Cases 3 and 4 designed to isolate the effects of the number of bounds used and of the spectral distribution from that of the accuracy of the upper bounds used. Thus in these tables, the best possible lower bounds obtainable from Equation (3.30), where the actual eigenvalues are used as upper bounds, are given along with the integral formulation upper bounds and their resulting lower bound sets. Again, within a cluster of closely spaced eigenvalues the error in these best possible lower bounds is seen to be comparable for a given number of upper bounds. One obvious effect of the number of upper bounds used is the increase in the accuracy of the lower bounds. A more subtle effect is the interaction with the effect of clustering. When upper bounds for all members of a cluster are used, there is a significant improvement in the accuracy of the lower bounds in that cluster which is greater than the improvement obtained upon adding a bound to an isolated eigenvalue. For example, examine the relative error changes down the columns of Table 3.3. When the third upper bound is added, the relative error in columns 1 and 2 drops sharply; the addition of the fourth upper bound cuts the error by a more typical rate. A similar phenomenon occurs in Table 3.4, columns 4-6.

One other source of error in these series approximations which must be mentioned is that of the numerical truncation errors inherent in summing numbers of disparate magnitudes and in taking smaller differences of larger numbers. Both problems occur in the use of the corrected truncation lower bounds, especially in bounding the higher eigenvalues. Any use of this method must take account of these sources of error by summing from small to large and using high precision arithmetic.

TABLE 3.1

Comparison of Truncation and Extremization

Lower Bounds for the Least Eigenvalue

γ	θ	0.1	1.0	10.	100.
	EV	5.058	2.421	1.8063	1.73177
0.1	LK	1.190(76.)	1.430(41.)	1.8014(.27)	1.72653(.30)
	LI	4.447(12.)	2.364(2.4)	1.7709(2.0)	1.69822(1.9)
	EV	4.211	3.142	2.5292	2.44333
1.0	LK	2.488(41.)	3.133(.27)	2.4877(1.6)	2.43646(.28)
	LI	3.947(6.3)	3.080(2.0)	2.5043(.99)	2.42059(.93)
	EV	1.806	1.454	1.2251	1.19037
10.	LK	1.801(.27)	1.430(1.6)	1.1901(2.9)	1.18666(.31)
	LI	1.771(2.0)	1.448(.37)	1.2246(.04)	1.18994(.04)
	EV	0.596	0.484	0.4100	0.39868
100.	LK	0.595(.30)	0.482(.28)	0.4087(.31)	0.39737(.33)
	LI	0.587(1.5)	0.483(.27)	0.4099(.01)	0.39867(<.001)

EV = actual eigenvalue

LK = best of Krein lower bounds, Equations 3.32

LI = iterated trace truncation lower bound, Equation 3.29

Figures in parentheses are percent relative errors.

TABLE 3.2

Comparison of Six-Term Upper Bounds from Integral and Differential Formulations with Lower Bound Sets

Case 1: $\gamma = 0.1$, $\theta = 100$							
ν	1.731772	3.469050	5.21637	6.9767	8.751	10.54	12.3
UD	1.731776	3.469163	5.21736	6.9804	8.767	10.58	
LD	1.731284	3.453456	5.10183	6.5369	7.625	8.34	9.43
UI	1.731772	3.469052	5.21642	6.9770	8.754	10.55	
LI	1.731301	3.454027	5.10578	6.5510	7.655	8.39	9.54
Case 2: $\gamma = 100$, $\theta = 0.1$							
ν	0.59643	1.298409	1.79655	2.5966	3.0140	3.8943	4.25
UD	0.59697	1.298409	1.80962	2.5966	3.0676	3.8943	
LD	0.59622	1.263957	1.65526	2.0044	2.1017	2.1796	2.24
UI	0.59644	1.298409	1.79844	2.5966	3.0364	3.8943	
LI	0.59627	1.290145	1.75801	2.3813	2.6311	2.9364	3.24
Case 3: $\gamma = 10.0$, $\theta = 10.0$							
ν	1.22511	6.283	11.34	12.57	13.79	18.85	23.9
UD	1.23884	8.165	12.52	14.79	24.63	27.76	
LD	1.22477	2.656	2.66	2.66	2.66	2.66	2.66
UI	1.22515	6.422	12.06	12.96	22.52	26.12	
LI	1.22503	6.038	8.29	8.41	8.78	8.80	8.83
Case 4: $\gamma = 0.1$, $\theta = 0.1$							
ν	5.058	6.283	7.508	12.57	17.62	18.85	20.1
UD	5.316	8.165	10.827	14.79	21.84	27.76	
LD	4.601	5.368	5.552	5.62	5.65	5.65	5.65
UI	5.088	6.422	7.879	12.96	19.87	26.12	
LI	4.950	6.022	6.936	8.33	8.64	8.70	8.72

ν = actual eigenvalues
UD = upper bounds, differential formulation LD = corresponding lower bounds
UI = upper bounds, integral formulation LI = corresponding lower bounds

TABLE 3.3

Bounds for the Spectrum with $\gamma = 10$, $\theta = 10$ with Percent Relative Errors

NT	ν_i	1.225109	6.28	11.34	12.6	13.8	18.8	23.9
1	UB	1.226067(+.0781)						
	LB	1.224566(-.0444)	4.63(-26)					
	BP	1.224566(-.0444)	5.97(-5.1)					
2	UB	1.226067(+.0781)	7.54(+20)					
	LB	1.224779(-.0270)	4.63(-26)	4.81(-58)				
	BP	1.225008(-.0083)	5.97(-5.1)	9.07(-20)				
3	UB	1.225232(+.0100)	7.54(+20)	12.31(+8.5)				
	LB	1.224809(-.0246)	5.74(-8.7)	6.25(-45)	6.4(-49)			
	BP	1.225049(-.0049)	6.09(-3.1)	9.07(-20)	10.3(-18)			
4	UB	1.225232(+.0100)	6.68(+6.3)	12.31(+8.5)	13.7(+8.8)			
	LB	1.224962(-.0121)	5.78(-8.0)	6.93(-39)	7.0(-44)	7.1(-48)		
	BP	1.225077(-.0027)	6.17(-1.8)	9.82(-13)	10.3(-18)	12.1(-12)		
5	UB	1.225145(+.0029)	6.68(+6.3)	12.06(+6.4)	13.7(+8.8)	22.5(+63)		
	LB	1.224967(-.0116)	6.02(-4.2)	7.56(-33)	7.7(-39)	7.9(-43)	7.9(-58)	
	BP	1.225096(-.0011)	6.24(-.74)	10.58(-6.7)	11.4(-9.4)	12.1(-12)	15.1(-20)	
6	UB	1.225145(+.0029)	6.42(+2.2)	12.06(+6.4)	13.0(+3.1)	22.5(+63)	26.1(+39)	
	LB	1.225032(-.0063)	6.04(-3.9)	8.29(-27)	8.4(-33)	8.8(-36)	8.8(-53)	8.8(-63)
	BP	1.225102(-.0007)	6.26(-44)	10.86(-4.3)	11.8(-6.1)	12.6(-8.3)	15.1(-20)	17.2(-28)
7	UB	1.225122(+.0010)	6.42(+2.2)	11.93(+5.2)	13.0(+3.1)	20.1(+46)	26.1(+39)	30.0(+25)
	LB	1.225036(-.0060)	6.12(-2.6)	8.70(-23)	8.9(-29)	9.3(-32)	9.4(-50)	9.4(-61)
	BP	1.225104(-.0005)	6.26(-.33)	10.97(-3.2)	12.0(-4.7)	12.9(-6.5)	15.7(-17)	17.2(-28)
10	UB	1.225113(+.0003)	6.31(+.59)	11.80(+4.0)	12.7(+.94)	17.4(+26)	24.7(+31)	27.2(+14)
	LB	1.225073(-.0030)	6.17(-1.7)	9.75(-14)	10.1(-20)	10.9(-21)	11.3(-40)	11.3(-53)
	BP	1.225107(-.0002)	6.28(-.11)	11.21(-1.2)	12.4(-1.7)	13.4(-2.4)	17.4(-7.4)	20.3(-15)

ν_i = actual eigenvalue i
NT = number of test functions used for upper bounds
UB = upper bounds from Galerkin method, integral formulation
LB = lower bounds based on NT upper bounds
BP = lower bounds based on NT actual eigenvalues

TABLE 3.4

Bounds for the Spectrum with $\gamma = 0.1$, $\theta = 0.1$ with Percent Relative Errors

NT	ν_i	5.0581	6.283	7.51	12.57	17.62	18.85	20.1
	UB	5.2223(+3.2)						
1	LB	4.4473(-12)	5.360(-15)					
	BP	4.4473(-12)	5.584(-11)					
	UB	5.2223(+3.2)	7.539(+20)					
2	LB	4.5931(-9.2)	5.360(-15)	5.77(-23)				
	BP	4.7805(-5.5)	5.584(-11)	7.13(-5.0)				
	UB	5.1370(+1.6)	7.539(+20)	8.78(+17)				
3	LB	4.6832(-7.4)	5.692(-9.4)	5.93(-21)	6.28(-50)			
	BP	4.9999(-1.2)	6.118(-2.6)	7.13(-5.0)	10.84(-14)			
	UB	5.1370(+1.6)	6.678(+6.3)	8.78(+17)	13.68(+8.9)			
4	LB	4.8172(-4.8)	5.736(-8.7)	6.42(-15)	6.87(-45)	6.98(-60)		
	BP	5.0317(-.52)	6.207(-1.2)	7.33(-2.4)	10.84(-14)	13.26(-25)		
	UB	5.0877(+.59)	6.678(+6.3)	7.88(+4.9)	13.68(+8.9)	19.87(+13)		
5	LB	4.8829(-3.5)	6.004(-4.4)	6.60(-12)	7.63(-39)	7.78(-56)	7.83(-59)	
	BP	5.0401(-.36)	6.231(-.84)	7.38(-1.7)	11.27(-10)	13.27(-25)	14.62(-22)	
	UB	5.0877(+.59)	6.422(+2.2)	7.88(+4.9)	12.96(+13)	19.87(+13)	26.12(+39)	
6	LB	4.9504(-21.)	6.022(-4.2)	6.94(-7.6)	8.33(-34)	8.64(-51)	8.70(-54)	8.7(-56)
	BP	5.0466(-.23)	6.249(-.54)	7.43(-1.1)	11.66(-7.2)	14.24(-19)	14.62(-22)	16.4(-19)
	UB	5.0702(+.24)	6.422(+2.2)	7.65(+1.9)	12.96(+3.1)	19.05(+8.1)	26.12(+39)	32.2(+61)
7	LB	4.9763(-1.6)	6.136(-2.3)	7.03(-6.4)	8.99(-28)	9.45(-46)	9.56(-49)	9.6(-52)
	BP	5.0516(-.13)	6.264(-.30)	7.46(-.61)	12.02(-4.4)	15.31(-13)	15.87(-16)	16.4(-19)
	UB	5.0639(+.11)	6.314(+.49)	7.58(+.92)	12.69(+.94)	18.76(+6.5)	24.74(+31)	31.1(+55)
10	LB	5.0217(-.72)	6.191(-1.5)	7.28(-3.0)	10.26(-18)	11.37(-35)	11.64(-38)	11.7(-42)
	BP	5.0555(-.05)	6.276(-.12)	7.49(-.24)	12.34(-1.8)	16.51(-6.3)	17.36(-7.9)	18.1(-9.7)

ν_i = actual eigenvalue i
NT = number of test functions used for upper bounds
UB = upper bounds from Galerkin method, integral formulation
LB = lower bounds based on NT upper bounds
BP = lower bounds based on NT actual eigenvalues

CHAPTER 4

LOWER BOUNDS FOR THE EIGENFREQUENCIES OF STEPPED ELASTIC BEAMS

4.1 Introduction and Literature Review

In this chapter, the integral equation lower bound technique is applied to the problem of determining the free vibration frequencies of stepped elastic beams. This problem is quite similar to that of Chapter 3 on heat conduction and string vibrations, the primary difference being the higher order of the associated differential operator.

The beam problem has been investigated in a number of ways. As in the cases of heat conduction (Chapter 3) and harmonic waves (Chapter 5), Lang and Nemat-Nasser have applied their stationary principle variational method. In[16] both smooth and improved test functions were used to approximate the displacement and bending moment; estimates and bounds for the frequencies in a variety of beam configurations were obtained. Their results on a cantilevered beam will be used in the first example problem of this chapter. A variation of Weinstein's method of intermediate problems [32,33], namely Bazley and Fox's method of truncation [34,35], was employed by Bickford [18] to obtain lower bounds for the frequencies of a simply supported stepped beam. He also obtained upper bounds by the traditional Rayleigh-Ritz method. His results will be used in the second example problem of this chapter.

A number of authors have used some results from the integral equation formulations of beam problems. Buckens [36] obtained lower bounds for the first two frequencies of a stepped simply supported beam by a decomposition of the beam into simpler subsystems to bound the least frequency, and by use of a trace identity to bound the second frequency. Janos [37] also uses integral equation formulations of two related string problems to obtain a geometric mean type inequality involving partial products of eigenvalues of the beam and the related strings. His method reduces to that of finding frequencies or appropriate bounds for two string problems to obtain two sided bounds for λ_1, $\lambda_1 \cdot \lambda_2$, $\lambda_1 \cdot \lambda_2 \cdot \lambda_3$, etc. His technique, however, does not give sharp results for even the lowest frequency. Integral equation bounds were used on a beam problem with random elastic support by Boyce and Goodwin [21]. They used the usual lower bound obtained by truncation of the trace identity for the second kernel iterate, noting that information about higher frequencies can be used to improve the bound, although they did not do so.

The numerical results in this chapter are obtained for two example problems. In sections 4.4-4.5 a three piece cantilever beam is used to compare the results of the integral equation lower bound technique to those of the variational method used by Lang and Nemat-Nasser [16]. In sections 4.6-4.7, a two piece simply supported beam is used to compare the integral equation lower bounds to those obtained by the method of truncation by Bickford [18]. First, the source of the eigenvalue problem and the formulation of the related integral equation are discussed in sections 4.2-4.3.

4.2 Formulation of the Eigenvalue Problem

The most economical beam model is that of the Euler beam, described by the partial differential equation

$$\frac{\partial^2}{\partial x^2}\left(\kappa(x)\frac{\partial^2 u}{\partial x^2}\right) = \rho(x)\frac{\partial^2 u}{\partial t^2} \tag{4.1}$$

with spatially varying material properties, stiffness κ and density ρ, and with appropriate boundary and initial conditions.

Separation of variables yields the eigenvalue problem for free vibrations

$$(\kappa(x)w'')'' = \lambda\rho w \tag{4.2}$$

Typical boundary conditions include the cantilever or fixed-free case

$$w(0) = w'(0) = 0 \qquad w''(1) = (\kappa w'')'(1) = 0 \tag{4.3}$$

and the simply supported or hinged-hinged case

$$w(0) = w''(0) = w(1) = w''(1) = 0 \tag{4.4}$$

For the stepped beam case, where the stiffness κ is piecewise continuous, continuity of displacement, slope, bending moment and shear force are assumed at points of discontinuity in stiffness.

4.3 Green's Functions and Integral Equation Formulation

The Green's functions for the operator

$$L[w] \equiv [\kappa(x)w'']'' \tag{4.5}$$

under the various boundary conditions are obtained by repeated integration of the equation

$$L[G] = \delta(x-y) \tag{4.6}$$

and application of the boundary conditions.

The integrations lead to the general Green's function

$$G(x,y) = w(0) + w'(0)x + \kappa w''(0)B_1(x) + (\kappa w'')''(0)B_2(x) + B_3(x,y) \tag{4.7}$$

where the functions B_i are given by the double integrals

$$B_1(x) = \int_0^x \int_0^s \frac{dt}{K(t)}\, ds$$

$$B_2(x) = \int_0^x \int_0^s \frac{tdt}{K(t)}\, ds \tag{4.8}$$

$$B_3(x,y) = \int_0^x \int_y^s \frac{t-y}{K(t)}\, dtds$$

It can be shown, however, that B_3 can be expressed in terms of B_1, B_2 and the Heaviside unit step function H by

$$B_3(x,y) = H(x-y)[B_2(x) - yB_1(x) - B_2(y) + xB_1(y)]. \tag{4.9}$$

When appropriate boundary conditions are applied, one obtains the Green's functions. Two of these are:

Cantilever case :

$$G_c(x,y) = \begin{cases} yB_1(x) - B_2(x) & 0 \leq x \leq y \leq 1 \\ xB_1(y) - B_2(y) & 0 \leq y \leq x \leq 1 \end{cases} \tag{4.10}$$

Simply supported case:

$$G_{ss}(x,y) = \begin{cases} Cxy + x(B_2(y) - B_1(y)) + (y-1)B_2(x) & 0 \leq x \leq y \leq 1 \\ Cxy + y(B_2(x) - B_1(x)) - (x-1)B_2(y) & 0 \leq y \leq x \leq 1 \end{cases}$$

$$\text{where } C = B_1(1) - B_2(1) \tag{4.11}$$

As usual, integral equation formulations are obtained from the Green's functions and symmetrization of the resulting kernels. That is,

$$k(x,y) \equiv \sqrt{\rho(x)}\, G(x,y) \sqrt{\rho(y)}$$

$$\psi(\cdot) \equiv \sqrt{\rho(\cdot)}\, w(\cdot) \tag{4.12}$$

$$\psi(x) = \lambda \int_0^1 k(x,y)\psi(y)dy$$

It should be noted that in the case of piecewise constant material properties, the functions B_1 and B_2 are piecewise defined polynomials, and thus the kernel k is a piecewise continuous polynomial in x and y which is simply, though arduously, square-integrable.

4.4 Sample Problem #1--Cantilever Case

Lang and Nemat-Nasser[16] analyze a three-piece beam problem under three cases of boundary conditions: cantilever, simply supported, and fixed-hinged. They also consider buckling problems and vibrations under compressive loads for the simply supported case. Of the cases they considered, the cantilever beam under no compressive load has the simplest Green's function. Thus, it is the most tractable example of a three piece beam for analysis by integral equation methods. In this section, the parametrization and nondimensionalizations in [16]

are followed and integral equation lower bounds are found for the material property combinations discussed in their article.

Suppose a beam of unit length has material properties given by

$$\kappa(x) = \begin{cases} \kappa_1 & b < |2x-1| \leq 1 \\ \kappa_2 & |2x-1| \leq b \end{cases}$$

$$\rho(x) = \begin{cases} \rho_1 & b < |2x-1| \leq 1 \\ \rho_2 & |2x-1| \leq b \end{cases} \tag{4.13}$$

where b is the length of center section of the beam.

The eigenvalue problem is nondimensionalized by the substitutions

$$s(x) = \kappa(x)/\bar{\kappa} \qquad d(x) = \rho(x)/\bar{\rho} \qquad \nu^2 = \lambda\bar{\rho}/\bar{\kappa} \tag{4.14}$$

where the average material properties $\bar{\rho}$ and $\bar{\kappa}$ are

$$\begin{aligned} \bar{\rho} &= \rho_1(1-b) + \rho_2 b \\ \bar{\kappa} &= \kappa_1(1-b) + \kappa_2 b \end{aligned} \tag{4.15}$$

The material property discontinuities are parametrized by

$$\gamma \equiv \kappa_2/\kappa_1 \qquad \text{and } \theta \equiv \rho_2/\rho_1 \tag{4.16}$$

We then are lead to the dimensionless eigenvalue problem

$$\begin{aligned} &(s(x)v'')'' - \nu^2 d(x)v = 0 \\ &v(0) = v'(0) = 0; \qquad v''(1) = (s(x)v'')'(1) = 0 \\ &v,\ v',\ sv'',\ (sv'')' \text{ continuous on } (0,1) \end{aligned} \tag{4.17}$$

For the results that follow, a center integral length of b = 1/2 is assumed.

The components of the Green's functions (4.10) are then given by the piecewise defined continuous polynomial:

$$B_1(t) = \begin{cases} \frac{1}{2s_1} t^2 & 0 \le t < \frac{1}{4} \\ \frac{1}{2s_1} [t^2 + (\frac{1-\gamma}{\gamma})(t-\frac{1}{4})^2] & \frac{1}{4} \le t \le \frac{3}{4} \\ \frac{1}{2s_1} [t^2 + (\frac{1-\gamma}{\gamma})((t-\frac{1}{4})^2 - (t-\frac{3}{4})^2)] & \frac{3}{4} < t \le 1 \end{cases} \tag{4.18}$$

$$B_2(t) = \begin{cases} \frac{1}{6s_1} t^3 & 0 \le t < \frac{1}{4} \\ \frac{1}{6s_1} [t^3 + (\frac{1-\gamma}{\gamma})((t-\frac{1}{4})^3 + \frac{3}{4}(t-\frac{1}{4})^2)] & \frac{1}{4} \le t \le \frac{3}{4} \\ \frac{1}{6s_1} [t^3 + (\frac{1-\gamma}{\gamma})((t-\frac{1}{4})^3 + \frac{3}{4}(t-\frac{1}{4})^2) & \\ - (t-\frac{3}{4})^3 - \frac{9}{4}(t-\frac{3}{4})^2)] & \frac{3}{4} < t \le 1 \end{cases} \tag{4.19}$$

Here $s_1 = \kappa_1/\overline{\kappa} = 1/(1+b(\gamma-1)) = 2/(1+\gamma)$.

Integration of the squared amplitude of the kernel over the unit square then yields the iterated kernel trace, written as a matrix product:

$$\mathrm{tr}(K_c^{(2)}) = \frac{1}{18\cdot 35\cdot 4^8}\left(\frac{1+\gamma}{\gamma(1+\theta)}\right)^2 \begin{bmatrix}\gamma^2 & \gamma & 1\end{bmatrix} \begin{bmatrix}54256 & 61456 & 17780\\ 61456 & 40936 & 7808\\ 17780 & 7808 & 1056\end{bmatrix} \begin{bmatrix}1\\ \theta\\ \theta^2\end{bmatrix} \tag{4.20}$$

For the continuous case, with $\gamma = \theta = 1$, $\mathrm{tr}(K_c^{(2)}) = 11/1680$. This gives the lower bound of $\underline{\nu}_1^{(0)} = 3.5154$ to the least frequency of $\nu_1 = 3.5160$, a relative error of -.017%. Lower bounds for the least frequency from Equation 2.8 and lower bounds for the least two frequencies from Equation 2.9 and upper bounds from [16] were calculated for the five combinations of material properties in [16]. The results are presented in Table 4.1.

4.5 Numerical Results and Discussion

The numerical results contained in Table 4.1 were obtained on a TI-57 calculator, carrying 11 decimal digits in accuracy. The results for $\underline{\nu}^{(0)}$ are based on the iterated kernel trace alone, and are accurate to the digits shown. The other lower bounds are based on the upper bound correction to the iterated kernel trace and, except where noted, the results as reported in [16]. In the exceptional case, where $\gamma = 100$ and $\theta = 1$, it can be seen that the reported numbers in [16] do not show a sufficient number of places to use in the upper bound correction. In fact, the upper bounds to four decimals are not upper bounds at all. The different extra digit assumptions in ν_N and $\overline{\nu}_R$ for this case were chosen to show the radical difference in the accuracy of lower bounds obtainable from upper bounds which agree to four places. The same

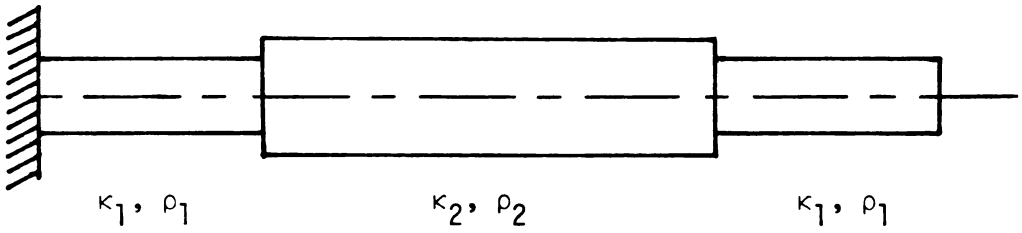

$$(\kappa u'')'' - \omega^2 \rho u = 0$$

$$u(0) = u'(0) = 0$$

$$u''(1) = (\kappa u'')'(1) = 0$$

FIGURE 4.1 Stepped cantilever beam - sample problem #1

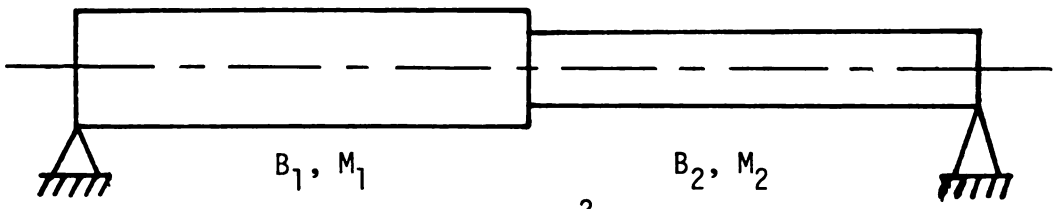

$$(Bu'')'' - \omega^2 Mu = 0$$

$$u(0) = u''(0) = 0$$

$$u(1) = u''(1) = 0$$

FIGURE 4.2 Stepped simply supported beam - sample problem #2

TABLE 4.1

Bounds for the Least Two Frequencies of a Stepped Cantilever Beam

γ	θ	ν	ν_N	$\bar{\nu}_R$	$\underline{\nu}^{(0)}$	$\underline{\nu}_N^{(2)}$	$\underline{\nu}_R^{(2)}$	$\underline{\nu}_B^{(2)}$
1	100	4.4138 28.9245	4.4139 29.1134	4.4139 29.1133	4.41315 --	4.41373 27.3154	4.41373 27.3154	4.41375 28.3070
3	100	3.3356 30.5004	3.3357 29.4830	3.4043 31.5635	3.33547 --	-- 25.9646	3.33558 6.30242	3.33559 30.01793
100	1	0.5889(18) 7.7567	0.5889(2) 8.18888	0.5889(5) 8.1888	0.588913 --	0.588917 6.99761*	0.588917 4.66540*	0.588918 7.57242*
100	3	0.6339 8.3985	0.6340 8.1872	0.6441 8.6512	0.633849 --	-- 3.60726	0.633853 1.26944	0.633854 4.72903
100	100	0.6875 10.5596	0.6875 9.2243	1.1207 33.2033	0.687489 --	-- 7.73167	0.687489 0.714242	0.687492 7.73167

Legend to Table 4.1: ν, ν_N, and $\bar{\nu}_R$ are the actual eigenvalues, new quotient approximations, and three-term Rayleigh-Ritz upper bounds taken from [16].

$\underline{\nu}^{(0)}$ is the lower bound from Equation 2.8.

$\underline{\nu}_N^{(2)}$, $\underline{\nu}_R^{(2)}$, $\underline{\nu}_B^{(2)}$ are the lower bounds based on ν_N, $\bar{\nu}_R$ and ν in Equation 4.30. Only the ν_N that are upper bounds were used.

*These figures are based on the assumed extra digits in ν, ν_N, $\bar{\nu}_R$ in parentheses. See discussion, section 4.5.

comment may be made on all entries in the last three columns pertaining to the least frequency; that is, they represent true lower bounds, but may not be the results which would be obtained had the full number of digits in the upper bounds been available. In the other chapters of this dissertation, all upper bounds used were calculated and all digits retained, rather than relying on figures tabulated elsewhere or rounded figures.

As can be seen in Table 4.1, in all these cases the first two frequencies are widely separated, accounting for the sharpness of the lower bounds $\underline{\nu}_1^{(0)}$. In cases of widely separated frequencies such as these, the dominant contribution to the kernel trace is that of the first frequency. Until that frequency is bounded very well from above, the lower bounds to the second frequency are quite poor. This is demonstrated by the marked difference in the lower bounds $\underline{\nu}_N$ and $\underline{\nu}_R$, where the bound from the new quotient approach is better than that from the Rayleigh-Ritz method.

4.6 Sample Problem #2--Simply Supported Case

Bickford [18] obtained lower bounds for the frequencies of a two-piece simply supported beam by Bayley and Fox's method of truncation [34]. In this section his development will be followed for the parametrization and nondimensionalization of the problem.

Suppose a beam of length ℓ has material properties given by

$$B(y) = \begin{cases} B_1 & 0 \leq y \leq y_1 \\ B_2 & y_1 < y \leq \ell \end{cases} \tag{4.21}$$

$$M(y) = \begin{cases} M_1 & 0 \leq y \leq y_1 \\ M_2 & y_1 < y \leq \ell \end{cases} \tag{4.21}$$

We then consider the eigenvalue problem

$$\begin{aligned} &\frac{d^2}{dy^2}\left(B(y)\frac{d^2u}{dy^2}\right) = \lambda M(y)u, \qquad 0 \leq y \leq \ell \\ &u(0) = \frac{d^2u}{dy^2}(0) = u(\ell) = \frac{d^2u}{dy^2}(\ell) = 0 \\ &u,\ \frac{du}{dy},\ B\frac{d^2u}{dy^2},\ \frac{d}{dy}\left(B\frac{d^2u}{dy^2}\right) \text{ continuous on } (0,\ell) \end{aligned} \tag{4.22}$$

This problem is transformed by the substitutions

$$\begin{aligned} &x = y/\ell \qquad b_0 = B_1/B_2 \qquad m_0 = M_2/M_1 \qquad \phi = (\ell^4 M_1/\pi^4 B_2)\lambda \\ &\text{and } v(x) = u(y(x)) \end{aligned} \tag{4.23}$$

to the dimensionless eigenvalue problem, where primes denote differentiation with respect to x,

$$\begin{aligned} &(bv'')'' = \pi^4 \phi m v \\ &v(0) = v''(0) = v(1) = v''(1) = 0 \\ &v, v', bv'', (bv'')' \text{ continuous} \end{aligned} \tag{4.24}$$

where $b = B/B_2$, $m = M/M_1$.

Bickford considers cases where $B_1 \geq B_2$ and $M_1 \geq M_2$, though with little modification, his analysis applies to all cases.

In applying the method of truncation, the underlying base problem of a uniform beam of unit stiffness and density has the eigenvalues and eigenfunctions

$$\phi_n^0 = n^4 \quad \text{and} \quad v_n^0 = \sqrt{2} \sin n\pi x \tag{4.25}$$

These functions form the basis of the Rayleigh-Ritz upper bounds reported in [18] and used in this section. Additional functions are used in generating the intermediate operators that approximate the actual operators of the problem. To this end, Bickford used the functions

$$p_i^1(x) = \sin(i\pi x/x_1)\cos(\pi x/2x_1)$$

$$q_i^1(x) = \sin(i\pi x) \tag{4.26}$$

for cases of discontinuous B and M respectively. In one case, he also uses the eigenfunctions r_i^1 of a uniform beam of length x_1 satisfying

$$r^{1\,iv} - \beta^4 r^1 = 0$$

$$r^1(0) = r^{1''}(0) = r^1(x_1) = r^{1'}(x_1) = 0 \tag{4.27}$$

for the approximation of the operator with discontinuous stiffness B.

The lower bounds from the truncation method are denoted by $\phi_i^{n,k,\ell}$ where the superscripts refer to the number n of base eigenfunctions and eigenvalues used, the number k of p_i^1 or r_i^1 used, and the number ℓ of q_i^1 used in forming the $k + \ell$ dimensional determinant equation to be solved for up to n lower bounds. If formally evaluated, solution of his determinant equation is equivalent to finding the zeros of a rational function whose poles are at the base eigenvalues.

Following his development, we find the iterated kernel trace and lower bounds in the form

$$\mathrm{tr}(K^{(2)}) = \sum_{1}^{\infty} \phi_i^{-2} \tag{4.28}$$

$$\underline{\phi}_1^{(0)} = (\mathrm{tr}(K^{(2)}))^{-\frac{1}{2}} < \phi_1 \tag{4.29}$$

$$\underline{\phi}_m^{(M)} = (\mathrm{tr}(K^{(2)}) - \sum_{n \neq m}^{M} \overline{\phi}_n^{-2})^{-\frac{1}{2}} < \phi_m \tag{4.30}$$

where the $\overline{\phi}_n$ are any upper bounds.

The value of $\mathrm{tr}(K^{(2)})$ in terms of system parameters and for $x_1 = 0.5$ is, in matrix product form,

$$\mathrm{tr}(K^{(2)}) = \frac{\pi^8}{6144 \cdot 9450 \cdot b_0^2} \begin{bmatrix} 1 & m_0 & m_0^2 \end{bmatrix} \begin{bmatrix} 791 & 710 & 175 \\ 710 & 1372 & 710 \\ 175 & 710 & 791 \end{bmatrix} \begin{bmatrix} 1 \\ b_0 \\ b_0^2 \end{bmatrix}. \tag{4.31}$$

Bickford's results, and the lower bounds for the least two eigenvalues based on the lower bounds of equations 4.29 and 4.30 using his upper bounds, are summarized in Table 4.2.

4.7 Discussion of Results--Problem #2

As can be seen in Table 4.2, the lower bounds based on the iterated kernel trace either with or without using upper bound information give comparable results in bounding the least eigenvalue to the far more expensive bounds from the method of truncation. In fact, the bounds computed from the trace and only the four low precision bounds of the twenty-four Rayleigh bounds are superior in all cases considered. These lower bounds would be even better if all digits and all of the upper bounds were available. In the second case, the bound for the second eigenvalue was based on a pessimistic extra digit in $\overline{\phi}_1^{R,24}$,

since the reported figure from [18] is not an upper bound. In all likelihood, the true upper bound was much better, and would have yielded a much better lower bound, though even the reported bound is quite good.

Also of note is the contrast between the results of the second and fourth cases, where the eigenvalues are the same. The coincidence of the spectra, which Bickford found remarkable, is due to the fact that the cases are duals of each other. That the results are the same when b_0^{-1} replaces m_0 and m_0^{-1} replaces b_0 is apparent from an examination of the equation for $tr(K^{(2)})$. As in all variational methods, discontinuities in coefficients associated with differentiated terms lead to poorer results. Thus when a dual problem is available, one should analyze the one which has a lesser discontinuity in the coefficient of the most highly differentiated term.

In the fourth case, with discontinuous stiffness, Bickford used the beam functions r_i^1 to improve the results obtained from using the p_i^1. The most accurate figures from each of these are those reported in Table 4.2. These bounds are much more expensive than those which were obtained for the dual second case, and far less accurate as well.

The question remains, however, whether a comparable computational investment in a Rayleigh-Ritz method, either through the use of more terms, improved test functions, or integral equation formulation, rather than in the method of truncation, would pay off by giving far better upper bounds and comparable lower bounds based on the iterated kernel trace.

TABLE 4.2

Bounds for the Least Two Squared Frequencies
of a Stepped Simply Supported Beam

b_0	m_0	$\phi^{32,16}$	$\phi^{64,32}$	$\overline{\phi}^{R,24}$	$\underline{\phi}^{(0)}$	$\underline{\phi}^{(4)}$
4	1	1.5198	1.5452	1.5945	1.57118	1.57298
		32.907	33.237	33.789	--	9.24096
		$\phi^{8,4}$	$\phi^{16,8}$	$\overline{\phi}^{R,24}$	$\underline{\phi}^{(0)}$	$\underline{\phi}^{(4)}$
1	0.5	1.3262	1.3262	1.3262	1.32394	1.32622
		23.111	23.111	23.111	--	22.9544*
		$\phi^{32,16,4}$	$\phi^{64,32,4}$	$\overline{\phi}^{R,24}$	$\underline{\phi}^{(0)}$	$\underline{\phi}^{(4)}$
2	0.5	1.7701	1.8212	1.8479	1.83768	1.84064
		33.132	33.199	33.215	--	17.6167
		$\phi_p^{64,32}$	$\phi_r^{64,32}$	$\overline{\phi}^{R,64}$	$\underline{\phi}^{(0)}$	$\underline{\phi}^{(1)}$
2	1.0	1.3129	1.3149	1.3281	1.32394	1.32394
		23.077	23.082	--	--	16.7328

Legend to Table 4.2

$\phi^{n,k,\ell}$ lower bounds from method of truncation

$\overline{\phi}^{R,N}$ N term Rayleigh-Ritz upper bounds

$\underline{\phi}^{(0)}$ Lower bound based on Equation 4.29

$\underline{\phi}^{(J)}$ Lower bounds based on Equation 4.30 and J upper bounds

*This bound computed using $\overline{\phi}_1^{R,24} = 1.32625$

CHAPTER 5

HARMONIC WAVES IN LAYERED COMPOSITES

5.1 Introduction and Literature Review

This chapter discusses the application of the integral equation lower bound technique to the problem of elastic waves propagating normal to the interfaces of layered composites with periodic structure. This problem was proposed by Lee [10] as a test case for variational methods to be applied to composites with periodic structures, and has been the subject of a number of papers [6,10-15]. Composite materials are highly dispersive in their wave propagation behavior, but Floquet theory shows that they admit certain stable wave systems, called Floquet waves, which do not disperse and retain their form relative to the periodic structure of the composite. In two- and three-dimensional lattices, the wave forms may only be determined approximately. However, for the one-dimensional composite formed by parallel plates, the wave forms for waves travelling normal to the interfaces can be determined exactly, and thus provides an objective measure of the accuracy of approximate methods.

In this chapter, numerical results are obtained for composites of two materials for a variety of material property combinations and wave numbers. Upper bounds are obtained by application of a Rayleigh-Ritz technique to the Sturm-Liouville eigenvalue problem with discontinuous

coefficients and quasi-periodic boundary conditions that arises from the application of Floquet theory to the governing partial differential equations. These are the upper bounds as discussed in [6]. Corresponding sets of lower bounds are obtained from the L^2 norm of the complex-valued kernel of the analogous integral equation. The actual eigenfrequencies were also obtained from the transcendental eigenvalue equation, and errors in the approximations are discussed.

5.2 Formulation of the Eigenvalue Problem

The governing partial differential equation for plane waves is the wave equation in each material subregion

$$\nabla^2 U(X,t) = c^2(X) \frac{\partial^2 U(X,t)}{\partial t^2} \tag{5.1}$$

where U may represent displacement, stress or strain and c is the spatially varying wave speed. Floquet waves are represented by a solution of the form

$$U(x,t) = u(X)e^{i(Q^T X - \omega t)} \tag{5.2}$$

where u(X) is a periodic function with the period of the composite, Q is a vector wave number giving the direction and wave length of the wave, and ω is the frequency.

For displacement waves travelling normal to the interfaces in a layered composite, Q and X are scalars, and insertion of (5.2) into (5.1) yields the eigenvalue problem for a cell of one period, the length of which is assumed to be l,

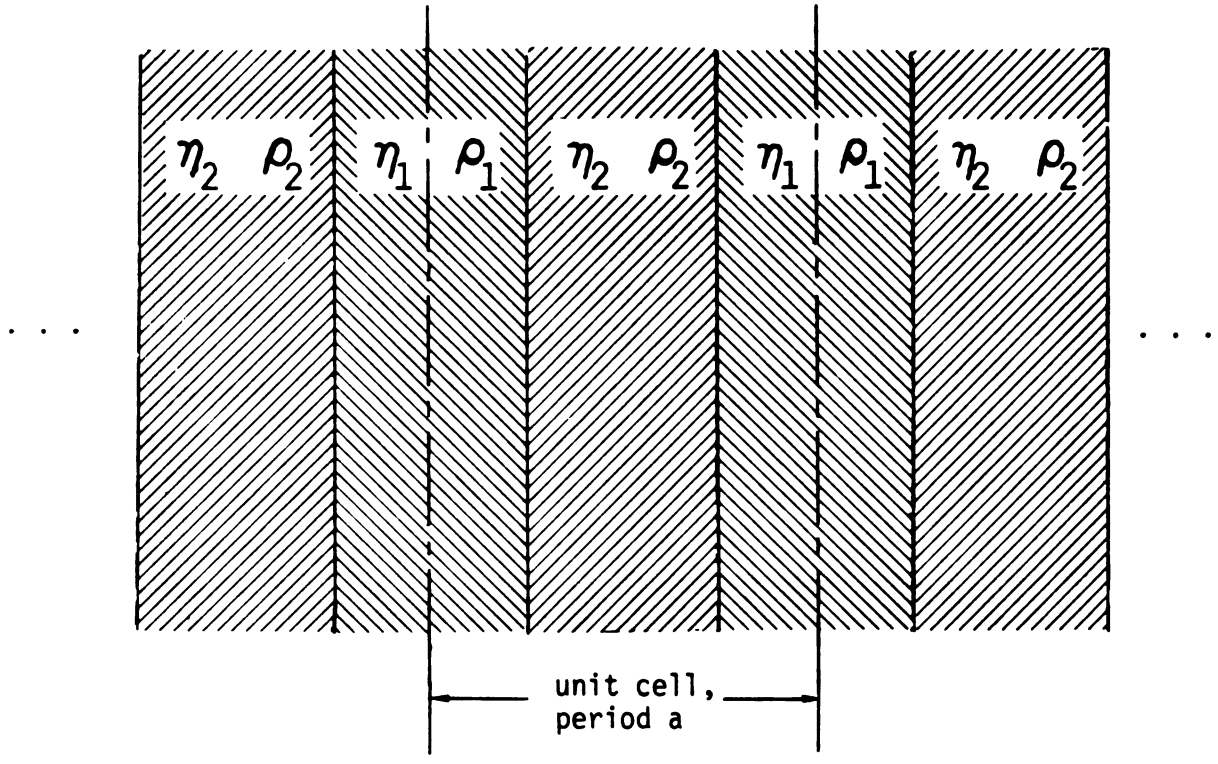

$$(\eta u')' + \omega^2 \rho u = 0$$

$$u(x+a) = e^{iQa} u(x)$$

$$\eta u'(x+a) = e^{iQa} \eta u'(x)$$

FIGURE 5.1 Layered composite with periodic structure

$$
\begin{aligned}
&(\eta(x)u')' + \omega^2\rho(x)u = 0 \\
&u(1) = e^{iQ}u(0) \qquad (\eta u')(1) = e^{iQ}(\eta u')(0)
\end{aligned}
\tag{5.3}
$$

The unit cell is chosen to start and end at the midpoint of two layers of the same material, and thus the second material layer is centrally located in the unit cell. Further, we require that certain interface conditions hold, namely continuity of displacement and stress,

$$u(x^-) = u(x^+) \text{ and } \eta(x^-)u'(x^-) = \eta(x^+)u'(x^+) \tag{5.4}$$

at the location x of any interface.

It has been shown that transformation of this problem to Liouville normal form by a substitution for the spatial variable x gives better results in the application of the Rayleigh-Ritz method for upper bounds [6]. Accordingly we set

$$t = \frac{1}{T}\int_0^x \eta^{-1}(s)ds, \qquad T = \int_0^1 \eta^{-1}(s)ds \tag{5.5}$$

$$f(t) = T^2\eta(x(t))\rho(x(t)) \tag{5.6}$$

$$v(t) = u(x(t)). \tag{5.7}$$

With these substitutions, the eigenvalue problem becomes

$$
\begin{aligned}
&\ddot{v} + \omega^2 f v = 0 \\
&v(1) = v(0)e^{iQ} \\
&\dot{v}(1) = \dot{v}(0)e^{iQ} \\
&v,\ \dot{v} \text{ continuous at interfaces}
\end{aligned}
\tag{5.8}
$$

The problem (5.3) may also be cast in terms of the stress $\sigma = \eta u'$, to be called the dual formulation:

$$(\rho^{-1}\sigma')' + \omega^2\eta^{-1}\sigma = 0$$

$$\sigma(1) = e^{iQ}\sigma(0);\ (\rho^{-1}\sigma')(1) = (\rho^{-1}\sigma')(0)\cdot e^{iQ} \tag{5.9}$$

σ, $\rho^{-1}\sigma'$ continuous at interfaces

The system (5.9) also admits transformation to Liouville normal form by the substitutions

$$s = \frac{1}{S}\int_0^x \rho(t)dt;\ S = \int_0^1 \rho(t)dt \tag{5.10}$$

$$g(s) = S^2\eta^{-1}(x(s))\rho^{-1}(x(s)) \tag{5.11}$$

$$w(s) = \sigma(x(s)) \tag{5.12}$$

With these substitutions, the dual problem becomes

$$\ddot{w} + \omega^2 g w = 0$$
$$w(1) = w(0)e^{iQ} \tag{5.13}$$
$$\dot{w}(1) = \dot{w}(0)e^{iQ}$$

w, $\dot{w}$ continuous at interfaces

Both the primal formulation (5.8) and the dual formulation (5.13) have the same eigenvalues, but their eigenfunctions differ. It has been shown in [6] that, depending on the relative magnitude of the discontinuities in the material constants, these formulations give differing eigenvalue bounds when a Rayleigh-Ritz procedure is applied to the corresponding variational formulations. This will be discussed further in section 5.5 on numerical results.

5.3 Integral Equation Formulation and Iterated Kernel Trace

The complex valued Green's function for either primal or dual formulation is the solution of the boundary value problem for each wave number $Q \neq 2n\pi$

$$-\frac{\partial^2 G}{\partial s^2}(s,t;Q) = \delta(s-t)$$

$$G(1,t;Q) = e^{iQ}G(0,t;Q) \tag{5.14}$$

$$\frac{\partial G}{\partial s}(1,t;Q) = e^{iQ}\frac{\partial G}{\partial s}(0,t;Q)$$

giving the solution

$$G(s,t;Q) = \begin{cases} \dfrac{(s-t)}{1-e^{iQ}} - \dfrac{e^{iQ}}{(1-e^{iQ})^2} & 0 \leq s \leq t \leq 1 \\ \dfrac{e^{iQ}(s-t)}{1-e^{iQ}} - \dfrac{e^{iQ}}{(1-e^{iQ})^2} & 0 \leq t \leq s \leq 1 \end{cases} \tag{5.15}$$

Note that G is hermitian, that is,

$$\overline{G}(t,s;Q) = G(s,t;Q) \tag{5.16}$$

Using this Green's function, one transforms the equations of the form of (5.8) and (5.13),

$$-\ddot{u} = \omega^2 h u$$

$$u(1) = e^{iQ}u(0) \qquad \dot{u}(1) = e^{iQ}\dot{u}(0) \tag{5.17}$$

to the integral equation

$$u(s) = \omega^2 \int_0^1 G(s,t;Q)h(t)u(t)dt. \tag{5.18}$$

The kernel of this equation, Gh, is not Hermitian, but an integral equation with a Hermitian kernel is obtained by the substitutions

$$\zeta(\cdot) = \sqrt{h}(\cdot)u(\cdot);$$

$$k_Q(s,t) = \sqrt{h(s)}G(s,t;Q)\sqrt{h(t)} \tag{5.19}$$

giving

$$\zeta(s) = \omega^2 \int_0^1 k_Q(s,t)\zeta(t)dt \equiv \omega^2 K_Q\zeta. \tag{5.20}$$

Further, the kernel of the second iterate K_Q^2 is

$$k_Q^{(2)}(s,r) = \int_0^1 k_Q(s,t)k_Q(t,r)dt = \int_0^1 k_Q(s,t)\overline{k}_Q(r,t)dt \tag{5.21}$$

giving

$$\begin{aligned} \mathrm{tr}(K_Q^2) &= \int_0^1 k_Q^{(2)}(s,s)ds \\ &= \int_0^1 \int_0^1 |k_Q(s,t)|^2 dtds. \end{aligned} \tag{5.22}$$

For the problem at hand, we define

$$C = -\frac{e^{iQ}}{(1-e^{iQ})^2} = \frac{1}{2(1-\cos Q)} \tag{5.23}$$

and thus

$$|k_Q(s,t)|^2 = h(s)h(t)C(C-|s-t| + (s-t)^2). \tag{5.24}$$

The value of $\mathrm{tr}(K_Q^2)$, which is the same as the L^2 norm of the kernel k_Q, will be obtained for the sample problem in the next section.

5.4 Sample Problem

We consider the sample problem of a layered composite consisting of equal amounts of two materials. The unit cell stiffness and density functions, then, are, for $0 \leq x \leq 1$

$$\eta(x) = \begin{cases} \eta_1 & |x - \frac{1}{2}| > \frac{1}{4} \\ \eta_2 & |x - \frac{1}{2}| < \frac{1}{4} \end{cases} \tag{5.25}$$

$$\rho(x) = \begin{cases} \rho_1 & |x - \frac{1}{2}| > \frac{1}{4} \\ \rho_2 & |x - \frac{1}{2}| < \frac{1}{4} \end{cases} \tag{5.26}$$

We then non-dimensionalize the problem by introducing the parameters

$$\gamma = \eta_2/\eta_1 \qquad \theta = \rho_2/\rho_1 \qquad \nu^2 = \omega^2\overline{\rho}/\overline{\eta} \tag{5.27}$$

where $\overline{\eta}$ and $\overline{\rho}$ are the average material properties. We then analyze the problem for the case $\overline{\eta} = \overline{\rho} = 1$, the frequencies for other cases following from the definition of ν.

Noting that the Liouville transformation changes the relative lengths of the two material regions, in either case we are led to a problem of the form (5.17), here repeated for convenience, and using eigenparameter ν^2,

$$\ddot{u} + \nu^2 h u = 0$$

$$u(1) = e^{iQ}u(0) \qquad \dot{u}(1) = e^{iQ}\dot{u}(0) \tag{5.28}$$

where the coefficient function h has the form

$$h(t) = \begin{cases} h_1 & |t - \frac{1}{2}| > \frac{1}{2}b \\ h_2 & |t - \frac{1}{2}| < \frac{1}{2}b \end{cases} \tag{5.29}$$

For the primal formulation,

$$\begin{aligned} b &= (1 + \gamma)^{-1} \\ h_1 &= (1 + \gamma)^3/(4\gamma^2(1 + \theta)) \\ h_2 &= \gamma\theta h_1 . \end{aligned} \tag{5.30}$$

For the dual formulation,

$$\begin{aligned} b &= \theta/(1 + \theta) \\ h_1 &= (1 + \gamma)(1 + \theta)/4\gamma\theta \\ h_2 &= h_1/\gamma\theta . \end{aligned} \tag{5.31}$$

In either case, one obtains the same value for $tr(K_Q^2)$, namely

$$tr(K_Q^2) = h_1^2 \frac{C}{6} [(6C-1)(1 + (\frac{h_2}{h_1} - 1)b)^2 + b^2(1-b)^2(1 - \frac{h_2}{h_1})^2] \tag{5.32}$$

or in terms of the parameters Q, γ, θ:

$$tr(K_Q^2) = (\frac{1+\gamma}{\gamma})^2[(\frac{2+\cos Q}{1-\cos Q})(1+\gamma)^2 + (\frac{1-\gamma\theta}{1+\theta})^2]/192(1-\cos Q) \tag{5.33}$$

Either of these are seen to reduce in the continuous case to

$$tr(K_Q^2) = \frac{C}{6}(6C-1) = \frac{2+\cos Q}{12(1-\cos Q)^2} \tag{5.34}$$

The transcendental equation for the eigenparameter ν in terms of Q, γ and θ is

$$4\sqrt{\gamma\theta}\cos Q = (1 + \sqrt{\gamma\theta})^2\cos\xi_1\nu - (1 - \sqrt{\gamma\theta})^2\cos\xi_2\nu \tag{5.35}$$

$$\text{where } \xi_1 = \frac{1}{2}\left(\frac{\sqrt{1+\gamma}}{1+\theta} + \frac{\sqrt{1+\gamma^{-1}}}{1+\theta^{-1}}\right) \tag{5.36}$$

$$\text{and } \xi_2 = \frac{1}{2}\left(\frac{\sqrt{1+\gamma}}{1+\theta} - \frac{\sqrt{1+\gamma^{-1}}}{1+\theta^{-1}}\right) \tag{5.37}$$

5.5 Numerical Results

Numerical results have been obtained for the sample problem on the Cyber 750 computer of the Computer Laboratory at Michigan State University. Upper bounds for the eigenparameter ν were obtained by applying a Rayleigh-Ritz procedure to both the primal and dual formulations of the problem. For this procedure, test functions of the form

$$u(t) = \sum_{n=-M}^{M} C_n e^{i(Q+2n\pi)t}$$

with M ranging from 0 to 6 provide sets of 1 to 13 upper bounds from each formulation.

Preliminary lower bounds to the least eigenparameter ν_1 were found from (5.33) and the lower bound (2.8). Increasing sets of lower bounds were obtained from the primal and dual upper bounds and the lower bounds (2.9). Additionally, lower bounds based on (2.9) and a merged set of upper bounds chosen from the primal and dual upper bound sets were also computed.

The actual eigenvalues were obtained from the eigenvalue equation (5.35) by using the best bounds obtained, searching these intervals for a sign change, and then using the secant method to converge on the roots. These roots were then used as upper bounds to generate the best possible lower bounds obtainable from Equation (2.9).

The lower bounds for the least eigenvalue for various combinations of γ and θ are in Tables 5.1 and 5.2 for Q = 1 and 3 respectively. These figures contain the actual eigenvalues, the preliminary lower bounds based on (2.8), the better of the primal and dual upper bounds based on test functions with M = 1 (three term approximations), and the lower bound based on the best bound set obtained from the primal and dual upper bounds with M = 1.

Lower bounds for the second eigenvalue for the same values of γ and θ as Tables 5.1 and 5.2 are presented in Tables 5.3 and 5.4 for Q = 1 and 3 respectively. These figures show the effect of using more and better upper bounds in the lower bound (2.9). The figures contain the actual second eigenvalues, lower bounds based on the better of the primal and dual upper bounds for M = 1 and M = 6, and the best possible lower bounds for the corresponding number of upper bounds.

A detailed examination of the upper and lower bounds for γ = 10, θ = 0.01 and Q = 1 and 3 are presented in Tables 5.5 and 5.6. The tabulated numbers, with percent relative errors, are: the actual eigenvalues; primal and dual upper bound sets; corresponding lower bound sets; lower bound sets based on choosing the best upper bounds from the primal and dual formulations; and the best possible lower bounds for the corresponding number of upper bounds.

5.6 Discussion of Results

An examination of Tables 5.1 and 5.2 shows that the preliminary lower bounds are very accurate for Q = 1 and less so for Q = 3. This is due to the relatively wide separation of the first two eigenvalues

in the former case and the lesser separation in the latter. In fact, the continuous cases, where the product $\gamma\theta = 1$, produce the least accurate lower bounds. This defect is remedied by use of some upper bound information, and the lower bounds obtained using this information have less than 0.4% error for all combinations of γ and θ studied.

An examination of Tables 5.3 and 5.4 on the second eigenvalue shows the marked increase in the accuracy of these lower bounds as more upper bound information is included. Of particular note are the cases where $\gamma\theta >> 1$, where the bounds based on the variational upper bounds are very poor, indicative of the poor performance of the upper bound techniques in these highly discontinuous cases. Clearly, the use of improved test functions with appropriate interface behavior may be worth the additional computational cost in such cases. The use of integral equation variational methods would also be of aid here, as is seen in Chapter 3 and Chapter 6. The best possible lower bounds shown in Tables 5.3 and 5.4 show how much better the lower bound technique could perform with good upper bounds, and thus provide a measure of how poor the upper bounds are.

Tables 5.5 and 5.6 allow comparison of the primal and dual upper bounds for the first seven eigenvalues. In Table 5.5, it is seen that the primal bounds are better than the dual, with the exception of the highest frequency estimated in each line. However in Table 5.6, it is seen that the primal is better for the odd numbered eigenvalues, the dual for the even. Similar analysis was applied to many combinations of material properties and wave numbers with the result that neither formulation was ever superior for the bounding of the whole

spectrum, further there were cases where the performance of primal and dual formulations were the opposite of that noted in Tables 5.5 and 5.6.

Also of note in Tables 5.5 and 5.6 is the performance of the lower bound technique, particularly when the better upper bounds were selected from the primal and dual bounds to obtain the lower bound sets. When these lower bounds are compared in accuracy to the best possible lower bounds, it is seen that, for at least the first half of the number of frequencies estimated, the performance of the lower bound technique is excellent. This reflects the accuracy of the corresponding upper bounds in this case with a relatively mild discontinuity, $\gamma\theta = 0.1$.

The results of more highly discontinuous cases which are not here tabulated are quite poor due to the inability of the Rayleigh-Ritz method based on the differential equation form with smooth test functions to cope with the important interface conditions and concomitant curvature changes in the true eigenfunctions. The mixed variational scheme of Nemat-Nasser [13] deals more successfully with these cases, and upper bounds he obtained, used in conjunction with the lower bound technique developed in Chapter 2, give better results. It is quite possible however that the more standard upper bound methods using either the integral equation formulation or improved test functions could perform as well as has been seen in Chapter 3 and Chapter 6. These methods were not tested on the case of harmonic waves.

TABLE 5.1

Lower Bounds to the Least Eigenvalue, Q = 1

γ \ θ		.01	.1	1	10	100
1	ν	.989296	.992457	1.000000	.992457	.989296
	$\underline{\nu}(0)$	.988987(-.031)	.992135(-.032)	.999563(-.044)	.992135(-.032)	.988987(-.031)
	$\overline{\nu}(3)$	.989432(+.014)	.992554(+.010)	1.000000(0.0)	.992554(+.010)	.989432(+.014)
	$\underline{\nu}(3)$	.989223(-.007)	.992401(-.006)	.999972(-.003)	.992401(-.006)	.989223(-.007)
10	ν	.574790	.574960	.570623	.558532	.555430
	$\underline{\nu}(0)$	.574538(-.044)	.574708(-.044)	.570438(-.032)	.558512(-.004)	.555420(-.002)
	$\overline{\nu}(3)$	.574835(+.008)	.574960(0.0)	.570678(+.010)	.562867(+.776)	.560541(+.920)
	$\underline{\nu}(3)$	.574771(-.003)	.574944(-.003)	.570591(-.006)	.558521(-.002)	.555427(-.001)
100	ν	.198020	.197961	.195900	.191294	.19015788
	$\underline{\nu}(0)$	.197933(-.044)	.197875(-.044)	.195839(-.031)	.191290(-.002)	.19015779(-4E-7)
	$\overline{\nu}(3)$	.198020(0.0)	.197977(+.008)	.195927(+.014)	.193054(+.920)	.192916(+1.45)
	$\underline{\nu}(3)$	.198014(-.003)	.197955(-.003)	.195886(-.007)	.191292(-.001)	.19015782(-1E-7)

ν = actual eigenvalue

$\underline{\nu}(n)$ = lower bound based on n upper bounds

$\overline{\nu}(n)$ = upper bound based on n term approximation

Figures in parentheses are percent relative errors.

TABLE 5.2

Lower Bounds to the Least Eigenvalue, Q = 3

γ	θ	.01	.1	1	10	100
1	ν	2.43272	2.51668	3.00000	2.51668	2.43272
	$\underline{\nu}^{(0)}$	2.37723(-2.3)	2.43893(-3.1)	2.61903(-12.7)	2.43893(-3.1)	2.37723(-2.3)
	$\overline{\nu}^{(3)}$	2.44111(+.35)	2.52350(+.27)	3.00000(0.0)	2.52350(+.27)	2.44111(+.35)
	$\underline{\nu}^{(3)}$	2.43031(-.10)	2.51335(-.13)	2.98992(-.34)	2.51335(-.13)	2.43031(-.10)
10	ν	1.69671	1.72488	1.44699	1.22159	1.18716
	$\underline{\nu}^{(0)}$	1.50101(-11.5)	1.50583(-12.7)	1.40228(-3.1)	1.22027(-.11)	1.18665(-.04)
	$\overline{\nu}^{(3)}$	1.69715(+.03)	1.72488(0.0)	1.45091(+.27)	1.27932(+4.7)	1.24802(+5.1)
	$\underline{\nu}^{(3)}$	1.69083(-.35)	1.71908(-.34)	1.44507(-.13)	1.22110(-.04)	1.18713(-.003)
100	ν	.594059	.584357	.481726	.408867	.397663
	$\underline{\nu}^{(0)}$	.518619(-12.7)	.516956(-11.5)	.470738(-2.3)	.408692(-.04)	.397659(-.001)
	$\overline{\nu}^{(3)}$	.594059(+0.0)	.584510(+.03)	.483389(.35)	.429825(+5.1)	.427772(+7.6)
	$\underline{\nu}^{(3)}$	.592063(-.34)	.582333(-.35)	.481250(-.10)	.408856(-.003)	.397661(-.0005)

ν = actual eigenvalue

$\underline{\nu}^{(n)}$ = lower bound based on n upper bounds

$\overline{\nu}^{(n)}$ = upper bound based on n term approximation

TABLE 5.3

Lower Bounds to the Second Eigenvalue, Q = 1

γ	θ	.01	.1	1	10	100
1	ν	5.47795	5.50546	5.28319	5.50546	5.47795
	$\underline{\nu}^{(3)}$	4.8904(-11)	5.0201(-8.8)	5.1744(-2.1)	5.0201(-8.8)	4.8904(-11.)
	$\underline{\underline{\nu}}^{(3)}$	5.4214(-1.0)	5.4226(-1.5)	5.1744(-2.1)	5.4226(-1.5)	5.4214(-1.0)
	$\underline{\nu}^{(13)}$	5.4409(-0.7)	5.4770(-.52)	5.2816(-.08)	5.4770(-.52)	5.4409(-0.7)
	$\underline{\underline{\nu}}^{(13)}$	5.4773(-.01)	5.5042(-.02)	5.2816(-.03)	5.5042(-.02)	5.4773(-.01)
10	ν	3.02855	3.03762	3.16542	5.72465	6.17207
	$\underline{\nu}^{(3)}$	2.8198(-6.9)	2.9751(-2.1)	2.8863(-8.8)	1.3356(-77.)	1.2747(-79.)
	$\underline{\underline{\nu}}^{(3)}$	2.9676(-2.0)	2.9751(-2.1)	3.1178(-1.5)	5.5705(-2.7)	6.1205(-.84)
	$\underline{\nu}^{(13)}$	3.0238(-1.6)	3.0367(-.03)	3.1490(-.52)	3.4048(-41.)	3.3080(-46.)
	$\underline{\underline{\nu}}^{(13)}$	3.0277(-.03)	3.0367(-.03)	3.1647(-.02)	5.7223(-.04)	6.1713(-.01)
100	ν	1.04618	1.04305	1.08474	2.12570	6.0930
	$\underline{\nu}^{(3)}$	1.0246(-2.1)	0.9712(-6.9)	0.9684(-11.)	0.4390(-79.)	0.3910(-94.)
	$\underline{\underline{\nu}}^{(3)}$	1.0246(-2.1)	1.0221(-2.0)	1.0735(-1.0)	2.1079(-.84)	5.8891(-3.3)
	$\underline{\nu}^{(13)}$	1.0459(-.03)	1.0414(-.16)	1.0774(-.07)	1.1393(-46)	0.5837(-90)
	$\underline{\underline{\nu}}^{(13)}$	1.0459(-.03)	1.0428(-.03)	1.0846(-.01)	2.1254(-.01)	6.0898(-.05)

ν = actual second eigenvalue

$\underline{\nu}^{(n)}$ = lower bound based on n upper bounds, selected from primal and dual

$\underline{\underline{\nu}}^{(n)}$ = lower bound based on n actual roots

TABLE 5.4

Lower Bounds to the Second Eigenvalue, Q = 3

γ	θ	.01	.1	1	10	100
1	ν	4.42974	4.22311	3.28319	4.22311	4.42974
	$\underline{\nu}^{(3)}$	4.2401(-4.3)	4.1019(-2.9)	3.2674(-.48)	4.1019(-2.9)	4.2401(-4.3)
	$\underline{\underline{\nu}}^{(3)}$	4.4083(-.48)	4.1955(-.65)	3.2674(-.48)	4.1955(-.65)	4.4083(-.48)
	$\underline{\nu}^{(13)}$	4.4280(-.04)	4.2215(-.04)	3.2830(-.005)	4.2215(-.04)	4.4280(-.04)
	$\underline{\underline{\nu}}^{(13)}$	4.4295(-.006)	4.2228(-.008)	3.2830(-.005)	4.2228(-.008)	4.4295(-.006)
10	ν	1.92006	1.88770	2.42812	5.06159	5.95724
	$\underline{\nu}^{(3)}$	1.9092(-.57)	1.8786(-.48)	2.3584(-2.9)	1.8944(-63)	1.8153(-70)
	$\underline{\underline{\nu}}^{(3)}$	1.9110(-.47)	1.8786(-.48)	2.4122(-.65)	4.9709(-1.8)	5.9129(-.74)
	$\underline{\nu}^{(13)}$	1.9299(-.006)	1.8876(-.005)	2.4272(-.04)	4.2081(-17)	4.4172(-26)
	$\underline{\underline{\nu}}^{(13)}$	1.9200(-.005)	1.8876(-.005)	2.4279(-.008)	5.0603(-.03)	5.9566(-.01)
100	ν	0.65014	0.66128	0.87718	2.05171	5.88552
	$\underline{\nu}^{(3)}$	0.6470(-.48)	0.6575(-.57)	0.8396(-4.3)	0.6252(-70)	0.5606(-90)
	$\underline{\underline{\nu}}^{(3)}$	0.6470(-.48)	0.6582(-.47)	0.8729(-.48)	2.0364(-.74)	5.7112(-3.0)
	$\underline{\nu}^{(13)}$	0.6501(-.005)	0.66124(-.006)	0.8768(-.04)	1.5213(-26)	0.8437(-86)
	$\underline{\underline{\nu}}^{(13)}$	0.6501(-.005)	0.66125(-.005)	0.8771(-.006)	2.0515(-.01)	5.8828(-.05)

ν = actual second eigenvalue

$\underline{\nu}^{(n)}$ = lower bound based on n upper bounds, selected from primal and dual

$\underline{\underline{\nu}}^{(n)}$ = lower bound based on n actual roots

TABLE 5.5

Bounds to the Spectrum with Q = 1, γ = 10, θ = 0.01

#	i	1	2	3	4	5	6	7	8
	ν_i	0.5747898	3.02856	4.2068	6.632	7.878	10.26	11.58	13.91
1	UP	0.5749596(+.030)							
	UD	0.5749596(+.030)							
	LP	0.5745377(-.044)	2.46917(-18)						
	LD	0.5745377(-.044)	2.46917(-18)						
	LB	0.5745377(-.044)	2.46917(-18)						
	BPL	0.5745377(-.044)	2.80793(-7.3)						
3	UP	0.5748347(+.008)	3.03557(+.23)	4.2422(+.84)					
	UD	0.5748510(+.011)	3.03877(+.34)	4.2270(+.48)					
	LP	0.5747706(-.003)	2.81780(-7.0)	3.4362(-18)	3.956(-40)				
	LD	0.5747706(-.003)	2.77542(-8.4)	3.3173(-21)	3.737(-44)				
	LB	0.5747713(-.003)	2.81979(-6.9)	3.4362(-18)	3.966(-40)				
	BPL	0.5747740(-.003)	2.96762(-2.0)	3.9282(-6.6)	5.614(-16)				
5	UP	0.5748085(+.003)	3.03115(+.09)	4.2172(+.25)	6.673(+.62)	8.075(+2.5)			
	UD	0.5748256(+.006)	3.03437(+.19)	4.2177(+.26)	6.691(+.89)	7.935(+.72)			
	LP	0.5747845(-.001)	2.94054(-2.9)	3.8211(-9.2)	4.709(-29)	4.879(-38)	5.057(-51)		
	LD	0.5747838(-.001)	2.88328(-4.8)	3.6184(-14)	4.214(-36)	4.300(-45)	4.398(-57)		
	LB	0.5747847(-.001)	2.94148(-2.9)	3.8246(-9.1)	4.719(-29)	4.879(-38)	5.071(-51)		
	BPL	0.5747862(-.001)	3.01406(-.49)	4.1342(-1.7)	6.049(-8.8)	6.722(-15)	8.118(-21)		
7	UP	0.5747985(+.002)	3.02974(+.04)	4.2112(+.11)	6.647(+.23)	7.924(+.59)	10.37(+1.1)	12.18(+5.1)	
	UD	0.5748148(+.004)	3.03256(+.13)	4.2142(+.17)	6.671(+.59)	7.913(+.44)	10.39(+1.2)	11.67(+.77)	
	LP	0.5747876(-.0004)	2.98693(-1.4)	4.0081(-4.7)	5.365(-19)	5.698(-28)	5.981(-42)	6.062(-48)	6.158(-56)
	LD	0.5747868(-.0005)	2.92791(-3.3)	3.769(-10.4)	4.572(-31)	4.706(-40)	4.809(-53)	4.830(-58)	4.866(-65)
	LB	0.5747877(-.0004)	2.98751(-1.4)	4.0107(-4.6)	5.376(-19)	5.711(-27)	6.000(-42)	6.065(-48)	6.181(-56)
	BPL	0.5747885(-.0002)	3.02320(-.18)	4.1794(-.65)	6.386(-3.7)	7.343(-6.8)	8.699(-15)	9.193(-21)	10.43(-25)

UP = upper bounds, primal formulation
UD = upper bounds, dual formulation
LP = lower bounds based on primal upper bounds
LD = lower bounds based on dual upper bounds
LB = lower bounds based on best upper bounds from primal/dual formulations
BPL= best possible lower bounds based on actual eigenvalues
ν_i = actual eigenvalues

TABLE 5.6

Bounds to the Spectrum with Q = 3, γ = 10, θ = 0.01

#	i	1	2	3	4	5	6	7	8
	ν_i	1.69671	1.92006	5.2022	5.6688	8.742	9.432	12.33	13.20
1	UP	1.72488(+1.7)							
	UD	1.72488(+1.7)							
	LP	1.50104(-12)	1.85733(-3.3)						
	LD	1.50104(-12)	1.85733(-3.3)						
	LB	1.50104(-12)	1.85773(-3.3)						
	BPL	1.50101(-12)	1.90245(-0.9)						
3	UP	1.69715(+.03)	1.92376(+.19)	5.3877(+3.6)					
	UD	1.69956(+.17)	1.92086(+.04)	5.3747(+3.3)					
	LP	1.68927(-.44)	1.90912(-.57)	4.1254(-21)	4.5836(-19)				
	LD	1.69083(-.35)	1.90489(-.79)	4.0568(-22)	4.4750(-21)				
	LB	1.69083(-.35)	1.90919(-.56)	4.2690(-18)	4.8464(-15)				
	BPL	1.69183(-.29)	1.91105(-.47)	4.3615(-16)	5.1715(-8.8)				
5	UP	1.69687(+.01)	1.92142(+.07)	5.2040(+.04)	5.7133(+1.1)	9.179(+5.0)			
	UD	1.69827(+.09)	1.92049(+.02)	5.2499(+.92)	5.6712(+.04)	9.071(+3.8)			
	LP	1.69481(-.11)	1.91759(-.13)	4.7582(-8.5)	5.0704(-11)	6.087(-30)	6.423(-32)		
	LD	1.69531(-.08)	1.91503(-.26)	4.6390(-11)	4.8485(-14)	5.637(-36)	5.869(-38)		
	LB	1.69547(-.07)	1.91790(-.11)	4.8808(-6.2)	5.2021(-8.2)	6.540(-25)	7.077(-25)		
	BPL	1.69580(-.05)	1.91838(-.09)	4.9815(-4.2)	5.3432(-5.7)	6.945(-21)	7.886(-16)		
7	UP	1.69678(+.004)	1.92067(+.03)	5.2033(+.02)	5.6913(+.40)	8.754(+.13)	9.648(+2.3)	13.19(+6.9)	
	UD	1.69777(+.06)	1.92036(+.02)	5.2333(+.60)	5.6703(+.03)	8.870(+1.5)	9.436(+.03)	12.80(+3.7)	
	LP	1.69593(-.05)	1.91910(-.05)	4.9950(-4.0)	5.3782(-5.1)	7.017(-20)	7.272(-23)	7.76(-23)	8.02(-39)
	LD	1.69607(-.04)	1.91720(-.15)	4.8424(-6.9)	5.1221(-9.6)	6.270(-28)	6.359(-33)	6.61(-46)	6.74(-49)
	LB	1.69621(-.03)	1.91929(-.04)	5.0575(-2.8)	5.4524(-3.8)	7.394(-15)	7.661(-19)	8.39(-32)	8.83(-33)
	BPL	1.69640(-.02)	1.91948(-.03)	5.1207(-1.6)	5.5455(-2.2)	7.873(-9.9)	8.255(-12)	9.33(-24)	10.29(-22)

CHAPTER 6

FREE VIBRATIONS OF A CIRCULAR MEMBRANE WITH RADIALLY STEPPED DENSITY

6.1 Introduction and Literature Review

In this chapter, integral equation methods are applied to the problem of determining the free vibration frequencies of a circular membrane with a discontinuous density. Upper bounds to the frequencies are found by applying Galerkin's method to both the differential and integral equation forms of the eigenvalue problem. Lower bounds are obtained by use of the trace identity and the aforementioned upper bounds. The actual eigenvalue equations are derived and solved numerically to assess the various bounds for their accuracy.

Considerable attention has been paid to the related problem of plates of stepped thickness in the acoustics literature [38-40]. The motivation behind this concern is the excellent directional radiative properties of such plates when used as high frequency transducers. The analysis of such plates by integral equation methods is possible, but much more complex than that of membranes just as the beam problem is more complex than the string problem. (See Chapters 3 and 4.) The membrane problem is chosen then as a more tractable illustrative case.

One numerical result on the stepped membrane problem was found in Krein's article [31] on eigenvalue extremization, where bounds were

found for the least frequency ranging from 3 percent to 10 percent in their spread. The mathematical theory and description of the free vibration eigenfunctions and eigenvalue equations have been discussed by Vodicka [41] and De [42], although no numerical examples of such membranes were given in their articles.

The numerical results in this chapter were obtained only for the axisymmetric modes of an axisymmetric circular membrane of two materials. The iterated kernel traces were found for modes with any number of nodal diameters, however. Bounds for the spectra and the actual eigenfrequencies were found for a number of internal radii and density ratios. The results suggest that the integral equation methods again give superior results in the upper bounds to the more traditional differential equation bounds and have the advantage of supplying lower bounds as well, with little additional effort.

6.2 Formulation of the Eigenvalue Problem

Small amplitude vibrations of a membrane clamped at its boundary may be modelled by the boundary value problem

$$\begin{aligned} T\nabla^2 W &= \rho \frac{\partial^2 W}{\partial t^2} \quad \text{on domain } D, \quad t \geq 0 \\ W &= 0 \quad \text{on boundary } \partial D, \quad t \geq 0 \end{aligned} \tag{6.1}$$

where the boundary curve is piecewise smooth, D is simply connected, T is the membrane tension, ρ the membrane density and W the transverse displacement.

Under the assumption that the tension and density are time-independent, the temporal and spatial dependence of the displacement may be separated by assuming a product solution

$$W(X,t) = w(X)f(t) \tag{6.2}$$

This yields an eigenvalue problem in the separation constant ω^2

$$\begin{aligned} f_{tt} + \omega^2 f &= 0 \\ T\nabla^2 w + \omega^2 \rho w &= 0 \quad \text{on } D \\ w &= 0 \qquad \text{on } \partial D \end{aligned} \tag{6.3}$$

In the particular case of a circular membrane under constant tension and with a radially symmetric density, the angular and radial dependence of the response may be further separated by assuming a product solution

$$w(r,\theta) = u(r)g(\theta) \tag{6.4}$$

This yields a separation constant η^2 and two sets of ordinary differential equations

$$\begin{aligned} g'' + \eta^2 g &= 0 \\ g(0) &= g(2\pi) \\ g'(0) &= g'(2\pi) \end{aligned} \tag{6.5}$$

and

$$
\begin{aligned}
&-((ru')' - \frac{\eta^2}{r} u) = \omega^2 \frac{r\rho(r)}{T} u \\
&\lim_{r\to 0} ru(r) = 0 \\
&u(R) = 0 \\
&u,\ ru' \text{ continuous}
\end{aligned}
\tag{6.6}
$$

where the primes denote differentiation with respect to the appropriate variables.

The system for g yields a solution for η^2, namely,

$$\eta = m;\ m = 0, 1, 2, \ldots \tag{6.7}$$

The parameter m represents the number of nodal diameters in the corresponding free vibration problem.

For notational convenience define the linear differential operators L_m by

$$L_m[u] = -(ru')' + \frac{m^2}{r} u, \quad m = 0, 1, 2, \ldots \tag{6.8}$$

Thus, separation of radial and angular dependence leads to a countable set of eigenvalue problems for the modes of vibration of the radially symmetric circular membrane of radius R:

$$
\begin{aligned}
&L_m[u] = \omega^2 r\rho(r)u/T, \quad m = 0, 1, 2, \ldots \\
&\lim_{r\to 0} ru(r) = 0,\ u(R) = 0,\ u,\ ru' \text{ continuous}
\end{aligned}
\tag{6.9}
$$

6.3 Integral Equation Formulation

System (6.9) may be recast in the form of integral equations by finding the corresponding Green's functions, that is, by solving

$$L_m[G_m(r;s)] = \delta(r-s)$$
$$\lim_{r\to 0} rG(r;s) = 0;\ G(R;s) = 0 \tag{6.10}$$

Then the eigenvalue problems can be written

$$u(r) = \frac{\omega^2}{T} \int_0^R G_m(r;s)s\rho(s)u(s)ds \tag{6.11}$$

This problem may be cast in a form with a symmetric kernel by multiplication by $\sqrt{r\rho(t)}$ and the substitutions

$$\psi(t) = \sqrt{t\rho(t)}\ u(t) \text{ and } k_m(r,s) = \sqrt{r\rho(r)}\ G_m(r;s)\ \sqrt{s\rho(s)}/T \tag{6.12}$$

yielding

$$\psi(r) = \omega^2 \int_0^R k_m(r,s)\psi(s)ds \tag{6.13}$$

The equation in this form is amenable to the techniques of analysis described in Chapter 2, and, as will be seen in the following, the kernel is symmetric and square-integrable.

6.4 Sample Problem

In the sequel, the problem of a circular membrane with a stepped radial density will be analyzed; numerical results are presented for the axisymmetric modes with m = 0.

Suppose the membrane density is given by

$$\rho(t) = \begin{cases} \rho_1 & 0 < t < A \\ \rho_2 & A < t < R \end{cases} \tag{6.14}$$

The average density $\bar{\rho}$ is then given by

$$\begin{aligned}\bar{\rho} &= \frac{1}{\pi R^2}\int_0^{2\pi}\int_0^R t\rho(t)dtd\theta \\ &= (A^2\rho_1 + (1-A^2)\rho_2)/A^2\end{aligned} \tag{6.15}$$

The problem is cast in terms of dimensionless parameters by the substitutions

$$r = t/R,\ a = A/R,\ \theta = \rho_2/\rho_1,\ d = \rho/\bar{\rho},\ \nu^2 = \omega^2\bar{\rho}/T \tag{6.16}$$

giving

$$d(r) = \begin{cases} (a^2 + \theta(1-a^2))^{-1} & 0 < r < a \\ \theta/(a^2 + \theta(1-a^2)) & a < r < 1 \end{cases} \tag{6.17}$$

and

$$L_m[u] = -(ru')' + \frac{m^2}{r}u = \nu^2 rd(r)u \tag{6.18}$$

The Green's functions for the operators L_m are

$$G_0(r,s) = \begin{cases} -\ln s & 0 \le r < s \le 1 \\ -\ln r & 0 \le s < r \le 1 \end{cases} \tag{6.19}$$

and for $m > 0$

$$G_m(r,s) = \begin{cases} r^m(s^{-m} - s^m)/2m & 0 \le r < s \le 1 \\ s^m(r^{-m} - r^m)/2m & 0 \le s < r \le 1 \end{cases} \tag{6.20}$$

The L^2 norms of the corresponding kernels are given by

$$||k_m||^2 = \int_0^1\int_0^1 rd(r)G_m(r,s)sd(s)dsdr \tag{6.21}$$

For the density d(r) given above, these norms are

$$||k_0||^2 = \frac{d_1^2}{32}\{1 + (\theta^2 - 1)[(1 - a^4) - 8a^4(\ln a)^2 + 4a^4 \ln a]$$

$$+ 8\theta(1 - \theta)[a^2(1 - a^2) - 2a^4(\ln a)^2 + 2a^4 \ln a]\} \qquad (6.22)$$

$$||k_1||^2 = \frac{d_1^2}{192}\{1 + (\theta^2 - 1)[6(1 - a^4) - 8(1 - a^6) + 3(1 - a^8)]$$

$$+ 6\theta(1 - \theta)a^4[24 \ln a - 24(1 - a^2) + 6(1 - a^4)]\} \qquad (6.23)$$

and for $m > 1$

$$||k_m||^2 = \frac{d_1^2}{4m^2(m+1)}\{\frac{m^2}{4(m+1)(m+2)} + (\theta^2 - 1)[\frac{1-a^4}{4} - \frac{1-a^{2m+4}}{m+2}$$

$$+ \frac{1-a^{4m+4}}{4(m+1)}] + \theta(1-\theta)a^{2m+2}[\frac{1-a^{2-2m}}{2-2m} - (1-a^2)$$

$$+ \frac{1-a^{2m+2}}{2m+2}]\} \qquad (6.24)$$

Note that in these formulae as a approaches 0 or 1 or as θ approaches 1 these formulae reduce to those of the continuous case, namely

$$||k_m||^2 = 1/(16(m+1)^2(m+2)); \quad m = 0, 1, 2, \ldots \qquad (6.25)$$

The differential equations $L_m[u] = \nu^2 rdu$ have as their solutions linear combinations of Bessel functions of order m in each material subinterval, namely

$$u_m(r) = \begin{cases} C_{11}J_m(\alpha r) + C_{12}Y_m(\alpha r) & 0 < r < a \\ C_{21}J_m(\beta r) + C_{22}Y_m(\beta r) & a < r < 1 \end{cases} \tag{6.26}$$

where $\alpha = \sqrt{d_1} \cdot \nu$ and $\beta = \sqrt{d_2} \cdot \nu$.

Using the four conditions, two boundary and two interface

$$\begin{aligned} &\lim_{r\to 0} ru_m(r) = 0,\ u_m(1) = 0 \\ &u_m,\ ru_m' \text{ continuous at } r = a \end{aligned} \tag{6.27}$$

a nontrivial solution is obtained when ν satisfies the equation

$$J_m(\alpha a\nu) = \frac{J_m'(\alpha a\nu)}{\sqrt{\theta}} \cdot \frac{J_m(\alpha\sqrt{\theta}a\nu)Y_m(\alpha\sqrt{\theta}\nu) - Y_m(\alpha\sqrt{\theta}a\nu)J_m(\alpha\sqrt{\theta}\nu)}{J_m'(\alpha\sqrt{\theta}a\nu)Y_m(\alpha\sqrt{\theta}\nu) - Y_m'(\alpha\sqrt{\theta}a\nu)J_m(\alpha\sqrt{\theta}\nu)}. \tag{6.28}$$

In the continuous case, these reduce to the familiar equations

$$J_m(\nu) = 0,\ m = 0, 1, 2, \ldots \tag{6.29}$$

Upper bounds to the eigenvalues may be obtained by applying Galerkin's method to either the integral or differential form of the problem. For the problem at hand, both methods were applied, using approximate eigenfunctions of a form appropriate for the axisymmetric modes:

$$u = \sum_1^n a_i \sin i\pi r / i\pi r \text{ in the differential form} \tag{6.30}$$

or

$$\psi = \sqrt{rd(r)}\, u \text{ in the integral form.} \tag{6.31}$$

The matrices for the method, in terms of the usual L^2 inner product are

$$(H)_{ij} = \langle ru_i', u_j' \rangle$$

$$(M)_{ij} = \langle \psi_i, \psi_j \rangle = \langle rd(r)u_i, u_j \rangle \tag{6.32}$$

$$(G)_{ij} = \langle \psi_i, K\psi_j \rangle .$$

The approximating eigenvalue problems then are:

$$Ha = \bar{\nu}^2 Ma \text{ in differential form}$$

and (6.33)

$$Ma = \bar{\nu}^2 Ga \text{ in integral form.}$$

6.5 Numerical Results

The numerical results in this section include the actual eigenvalues and both upper and lower bounds obtained by implementing the following procedure on the Prime 750 computer of the Case Center for Computer Aided Design at Michigan State University:

1. Generate increasing sets of upper bounds and corresponding lower bound sets from the Galerkin methods and equation (2.9).
2. Use the bounds generated to solve the actual eigenvalue equation by
   a. finding an interval where the equation has a sign change
   b. applying the secant method until the root is found
3. Use the actual eigenvalues to generate the best possible lower bounds obtainable from equation (2.9) and to compute relative errors.

Table 6.1 contains lower bounds to the least frequency for a number of internal radii and density ratios. These bounds were obtained from the kernel norm alone, using none of the upper bound information.

Tables 6.2 through 6.4 contain bounds to the spectrum of 3 cases of internal radius and density ratios, as well as the actual eigenvalues and percent relative errors of the bounds. The numbers tabulated are the upper bounds from both the integral and differential equation based Galerkin method, the lower bounds based on the integral upper bounds, and the best possible lower bounds, based on using the actual eigenvalues as bounds.

6.6 Discussion of Results

Examination of Table 6.2 shows that the upper bounds from the integral equation formulation are clearly superior to those from the differential equation formulation. However, both methods have difficulty coping with highly discontinuous cases. The superior performance of the integral formulation stems from the iteration of the test functions with the kernel, yielding essentially improved test functions having more of the properties of the actual eigenfunctions at the interface.

Examination of Table 6.1 shows that the preliminary lower bound based on knowledge only of the kernel norm are quite accurate, with relative errors ranging from 0.4 percent to 2 percent in the cases studied. The accuracy of this bound depends on the spectral structure, and for the cases studied the least frequency is well separated from the higher frequencies, yielding good lower bounds.

Examination of Tables 6.2, 6.3 and 6.4 shows that accurate lower bounds can be obtained provided that good upper bounds are used. The accuracy of the lower bounds for higher frequencies depends primarily on the accuracy of the upper bounds to the lesser frequencies. Given a good upper bound to the lower frequencies, the effects of eigenvalue spacing can be seen, especially in Table 6.2, where the actual frequencies come in closely spaced pairs after the isolated initial frequency. The lower bounds to each of the close pairs are of comparable accuracy, though the first lower bound obtained for the higher of the frequencies is better than the comparable bound for the lower of a pair; this is the effect of clustering on lower bound accuracy.

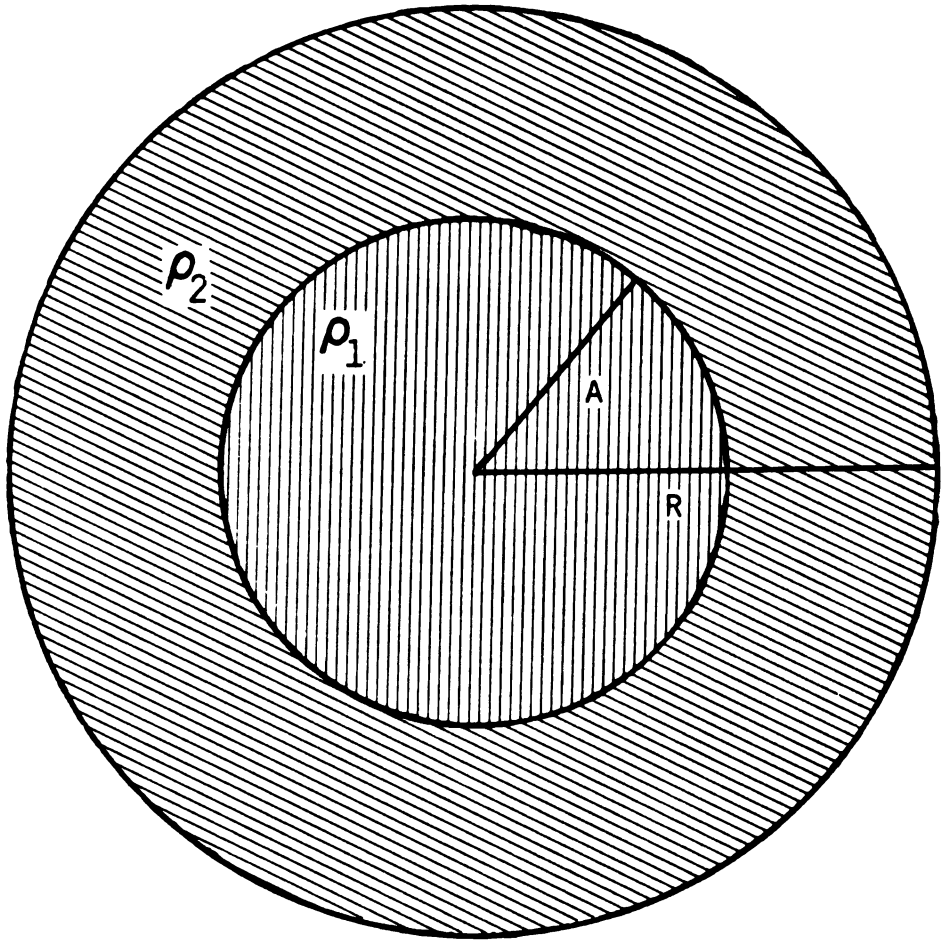

$$(ru')' - \frac{m^2}{r} u + \omega^2 \frac{r\rho}{T} u = 0$$

u, ru' continuous
u(0) finite, u(R) = 0
m = # of nodal diameters

FIGURE 6.1 Circular membrane with radially stepped density

TABLE 6.1

Bounds to the Least Frequency of the
Two-Piece Circular Membrane

a	θ	10	3	1/3	1/10
.1	ν	2.43282	2.42571	2.33789	2.09196
	UD	2.44599(+.54)	2.43715(+.47)	2.34503(+.30)	2.16144(+3.3)
	UI	2.43496(+.09)	2.42765(+.08)	2.33848(+.03)	2.10638(+.69)
	LØ	2.40815(-1.0)	2.40067(-1.0)	2.30659(-1.3)	2.05683(-1.7)
.5	ν	3.02808	2.83469	1.91760	1.61114
	UD	3.39475(+12)	2.97186(+4.8)	1.92658(+.47)	1.63398(+1.4)
	UI	3.06703(+1.3)	2.85978(+.89)	1.91852(+.05)	1.61259(+.09)
	LØ	3.00730(-.7)	2.804397(-1.1)	1.90554(-.63)	1.60399(-.44)
.7	ν	3.72529	3.09024	2.01280	1.84025
	UD	4.36498(+17)	3.18748(+31.)	2.01352(+.04)	1.84090(+.04)
	UI	3.88142(+4.2)	3.11528(+.81)	2.01288(+.004)	1.84027(+.001)
	LØ	3.67186(-1.4)	3.03337(-1.8)	1.99646(-.81)	1.82659(-.74)
.9	ν	3.87949	2.81390	2.25019	2.19328
	UD	3.92151(+1.1)	2.82612(+.43)	2.25681(+.29)	2.19952(+.28)
	UI	3.89011(+.27)	2.81613(+.08)	2.25132(+.05)	2.19434(+.05)
	LØ	3.80068(-2.0)	2.77939(-1.2)	2.22614(-1.1)	2.17003(-1.1)
.95	ν	3.28768	2.62759	2.32573	2.29739
	UD	3.30066(+.39)	2.63647(+.34)	2.33318(+.32)	2.30471(+.32)
	UI	3.29001(+.07)	2.62913(+.06)	2.32701(+.06)	2.29865(+.05)
	LØ	3.24764(-1.2)	2.59826(-1.1)	2.30030(-1.1)	2.27230(-1.1)

ν = actual least frequency
UD = upper bound, differential formulation
UI = upper bound, integral formulation
LØ = truncation lower bound, Equation 2.8

TABLE 6.2

Bounds for the Spectrum with a = .1, θ = .01

# terms	i	1	2	3	4	5	6	7
	ν_i	1.2066	4.47	5.76	9.33	10.3	14.0	15.0
1	UD	1.5308(+27)						
	UI	1.2325(+2.1)						
	LI	1.2042(-.20)	2.21(-51)					
	LB	1.2042(-.20)	4.05(-9.3)					
2	UD	1.3923(+15)	5.25(+17)					
	UI	1.2116(+.42)	4.76(+6.6)					
	LI	1.2055(-.09)	3.05(-32)	3.19(-45)				
	LB	1.2058(-.06)	4.05(-9.3)	5.37(-6.8)				
3	UD	1.3071(+8.3)	4.98(+11)	9.99(+73)				
	UI	1.2082(+.13)	4.63(+3.7)	9.42(+64)				
	LI	1.2057(-.07)	3.58(-19)	3.97(-31)	4.00(-57)			
	LB	1.2064(-.02)	4.35(-2.7)	5.37(-6.8)	7.64(-18)			
4	UD	1.2665(+5.0)	4.80(+7.3)	9.70(+68)	14.5(+55)			
	UI	1.2073(+.06)	4.58(+2.5)	8.99(+56)	13.1(+41)			
	LI	1.2058(-.07)	3.84(-14)	4.48(-22)	4.54(-51)	4.56(-56)		
	LB	1.2065(-.01)	4.40(-1.6)	5.53(-4.0)	7.64(-18)	8.86(-14)		
5	UD	1.2397(+2.7)	4.71(+5.4)	9.44(+64)	14.1(+51)	18.6(+80)		
	UI	1.2069(+.02)	4.55(+1.9)	8.42(+46)	11.7(+25)	16.6(+61)		
	LI	1.2059(-.06)	4.00(-10)	4.88(-15)	4.99(-46)	5.02(-51)	5.03(-64)	
	LB	1.2066(-.004)	4.44(-.73)	5.65(-1.9)	8.34(-11)	8.86(-14)	10.8(-23)	
10	UD	1.2080(+.11)	4.54(+1.5)	8.04(+40)	10.7(+14)	15.2(+47)	20.1(+43)	25.1(+67)
	UI	1.2066(+4E-4)	4.47(+.14)	5.96(+3.4)	9.71(+41.)	14.5(+41)	19.4(+38)	24.1(+61)
	LI	1.2064(-.015)	4.36(-2.5)	5.52(-4.1)	7.10(-24)	7.58(-27)	7.67(-45)	7.70(-49)
	LB	1.2066(-6E-4)	4.46(-.11)	5.74(-.29)	9.15(-1.9)	10.0(-2.8)	12.9(-8.3)	13.5(-10)

UD = upper bounds, differential formulation
UI = upper bounds, integral formulation
LI = lower bounds from UI and Equation 2.9
LB = lower bounds from ν_i and Equation 2.9
Figures in parentheses are percent relative errors; errors <.001 are in exponential format $\pm$ nE $\pm$ m = $\pm$ n·10$^{\pm m}$.

TABLE 6.3

Bounds for the Spectrum with a = .7, θ = 10,000

	i	1	2	3	4	5	6	7
# terms	ν_i	4.01241	11.316	18.75	26.2	33.7	41.2	48.6
1	UD	6.1407(+53)						
	UI	4.0480(+.89)						
	LI	3.9937(-.46)	8.339(-26)					
	LB	3.9937(-.46)	10.83(-4.4)					
2	UD	4.5451(+13)	85.43(+654)					
	UI	4.0143(+.05)	12.84(+13)					
	LI	4.0031(-.23)	10.57(-6.6)	12.33(-34)				
	LB	4.0093(-.08)	10.83(-4.4)	17.06(-910)				
3	UD	4.1229(+2.8)	34.05(+201)	289.9(+1445)				
	UI	4.0124(+.001)	11.87(+4.9)	96.04(+412)				
	LI	4.0066(-.15)	10.82(-4.4)	14.49(-23)	14.50(-45)			
	LB	4.0114(-.02)	11.15(-1.5)	17.06(-9.0)	22.8(-13)			
4	UD	4.0272(+.36)	19.37(+71)	224.5(+1097)	428.7(+1535)			
	UI	4.0124(+5E-4)	11.46(+1.3)	26.63(+42)	264.2(+908)			
	LI	4.0091(-.08)	10.90(-3.7)	16.09(-14)	16.7(-36)	16.7(-51)		
	LB	4.0120(-.01)	11.24(-.65)	17.92(-4.4)	22.8(-13)	28.1(-17)		
5	UD	4.0192(+.17)	14.07(+24)	124.2(+562)	299.1(+1041)	676(+1907)		
	UI	4.0124(+4E-4)	11.32(+.08)	21.18(+13)	197.0(+651)	334(+890)		
	LI	4.0106(-.05)	11.02(-2.6)	16.96(-9.5)	19.4(-26)	19.4(-42)	19.4(-53)	
	LB	4.0122(-.005)	11.28(-.34)	18.30(-2.4)	24.1(-8.0)	28.1(-17)	33.1(-20)	
10	UD	4.0138(+.03)	11.354(+.34)	19.30(+2.9)	58.2(+122)	24.9(+638)	507(+1133)	708(+1355)
	UI	4.0124(+2E-5)	11.316(+.001)	18.76(+.006)	26.7(+1.9)	45.0(+33)	244(+493)	467(+861)
	LI	4.0120(-.01)	11.25(-.62)	17.96(-4.2)	23.1(-11.7)	27.4(-18)	28.4(-31)	28.4(-42)
	LB	4.0124(-7E-4)	11.311(-.04)	18.69(-.33)	25.9(-1.2)	32.6(-3.2)	38.5(-6.4)	43.3(-11)

UD = upper bounds, differential formulation
UI = upper bounds, integral formulation
LI = lower bounds from UI and Equation 2.9
LB = lower bounds from ν_i and Equation 2.9
Figures in parentheses are percent relative errors; errors < .001 are in exponential format $\pm$ nE $\pm$ m = $\pm$ n·10$^{\pm m}$.

TABLE 6.4

Bounds for the Spectrum with a = .9, θ = 100

	i	1	2	3	4	5	6	7
# terms	ν_i	6.74445	12.113	20.85	27.4	35.0	42.7	49.1
1	UD	9.47910(+41)						
	UI	8.06463(+20)						
	LI	6.56529(-2.6)	7.587(-37)					
	LB	6.56529(-2.6)	11.615(-4.1)					
2	UD	8.94939(+33)	17.414(+44)					
	UI	7.17640(+6.4)	13.389(+11)					
	LI	6.66377(-1.2)	8.875(-27)	9.36(-55)				
	LB	6.71510(-.43)	11.615(-4.1)	18.52(-11)				
3	UD	8.46972(+26)	15.144(+25)	30.72(+47)				
	UI	6.88481(+2.1)	12.502(+3.2)	28.51(+37)				
	LI	6.70154(-.64)	10.220(-16)	11.76(-44)	11.8(-57)			
	LB	6.73327(-.17)	11.912(-1.7)	18.52(-11)	23.6(-14)			
4	UD	8.02866(+19)	13.912(+15)	29.00(+39)	45.4(+66)			
	UI	6.80178(+.85)	12.284(+1.4)	27.31(+31)	43.4(+59)			
	LI	6.71356(-.46)	10.973(-9.4)	13.89(-33)	14.1(-48)	14.1(-60)		
	LB	6.73946(-.07)	12.021(-.76)	19.64(-5.8)	23.6(-14)	28.9(-17)		
5	UD	7.65624(+14)	13.216(+9.1)	28.13(+35)	43.8(+60)	60.0(+71)		
	UI	6.77262(+.42)	12.208(+.78)	26.82(+29)	41.5(+52)	56.7(+62)		
	LI	6.71832(-.39)	11.335(-6.4)	15.46(-26)	15.8(-42)	15.9(-55)	15.9(-63)	
	LB	6.74178(-.04)	12.064(-.41)	20.16(-3.3)	25.0(-8.5)	28.9(-17)	33.8(-21)	
10	UD	6.82650(+1.2)	12.216(+.85)	26.53(+27)	39.7(+45)	50.9(+45)	63.7(+49)	78.6(+60)
	UI	6.74482(+.01)	12.117(+.03)	23.12(+11)	28.5(+4.3)	43.3(+24)	58.9(+38)	74.8(+52)
	LI	6.73356(-.16)	11.914(-1.6)	19.63(-5.9)	21.4(-22)	23.1(-45)	23.4(-45)	23.5(-52)
	LB	6.74408(-.01)	12.106(-.06)	20.75(-.50)	27.0(-1.4)	33.7(-3.6)	39.6(-7.3)	43.5(-11)

UD = upper bounds, differential formulation
UI = upper bounds, integral formulation
LI = lower bounds from UI and Equation 2.9
LB = lower bounds from ν_i and Equation 2.9
Figures in parentheses are percent relative errors; errors < .001 are in exponential format $\pm$ nE $\pm$ m = $\pm$ n·10$^{\pm m}$.

CHAPTER 7

SUMMARY AND SUGGESTIONS FOR FURTHER STUDY

7.1 Summary

As has been seen in the previous chapters of this dissertation, integral equation based approximate methods are quite effective in bounding the eigenvalues of systems with discontinuous coefficients.

The integral equation formulation of the Galerkin method leads to superior upper bounds to those obtained using the differential equation formulation. It is reasonable to expect that the results of other approximate methods applied to the differential formulation would be improved by using their integral equation formulations as well.

A further advantage of analyzing eigenvalue problems in integral equation form is the availability of the readily computed corrected truncation lower bounds from the trace identities. These bounds complement any set of upper bounds and by their convergence behavior give insight into the distribution of the spectrum as well.

There are, of course, some deficiencies in the integral equation approach. Of primary importance is the fact that in truly multi-dimensional problems over finite regions the Green's function necessary for integral equation formulation cannot be expressed in a closed form. Thus it is difficult to transform the differential equations to integral equations in a form amenable to computation. Secondarily,

the numerical roundoff and truncation errors inherent in applying the corrected truncation lower bounds from the trace identities on machines with finite precision must be dealt with effectively. This latter problem can be addressed by careful programming and the use of high precision arithmetic.

7.2 Suggestions for Further Study

The problem of eigenfunction approximation in discontinuous systems by integral equation methods is certainly deserving of consideration. Particularly of interest here is the application of the iterated Galerkin method [27], where the eigenfunctions are expressed in an expansion of test functions of the form $K\phi_i$ rather than ϕ_i, using the same coefficients as those determined for the expansion in the ϕ_i. That is, if the Galerkin expansion of the nth eigenfunction is given by

$$\hat{\psi} = \Sigma a_{ni}\phi_i,$$

the iterated Galerkin expansion is given by $K\hat{\psi}_n$, or

$$\hat{\psi}_n = \hat{\lambda}_n \Sigma a_{ni} K\phi_i.$$

The results of the latter expansion will generally be superior to that of the former, since iteration with the kernel gives functions which better satisfy the conditions at material interfaces than non-iterated functions. Further, this method requires little extra computation, since the $K\phi_i$ must be determined in order to obtain the Galerkin matrices.

Also of interest in both eigenvalue and eigenfunction determinations would be the results of other approximate methods in integral equation form such as collocation [26,43], the Nyström method [44,45] or finite element type approaches using hybrid elements appropriate for the material properties of the various subregions [10].

Most importantly, these integral equation based methods should be extended to problems in truly multidimensional systems where the Green's function may only be approximately determined. Likely candidates for approximation of the Green's function in complicated geometries are truncations of series representations (appropriate for Galerkin type methods) or finite difference or finite element static impulse responses (appropriate for collocation or Nyström methods). Also possible would be experimental determinations of the Green's function. It should be noted that the use of such procedures is equivalent to placing additional constraints on the dynamics of the systems in question and thus lower bounds which are based on traces of approximate kernels with generally raised eigenvalues need not be lower bounds to the true eigenvalues of the systems in question. They however are still of some use in assessing the accuracy of the upper bounds to the eigenvalues of the approximate kernels.

At the present stage of development, the user of the methods of this dissertation needs a fairly sophisticated understanding of the methods of integral equations and how their problem can be placed in the context of linear integral equations with time invariant boundary conditions. The software development for the example problems of this

project used many common modules, but required ad hoc sections for the various Green's functions, Galerkin test functions and inner product matrix evaluations. In addition, the iterated kernel traces that were found either by hand or symbolic manipulation computer programs in a parametric form were programmed in as formulae rather than being numerically determined. Further development of these algorithms so that they could be implemented on a computer for a non-sophisticated user thus would also be a fruitful area of investigation.

LIST OF REFERENCES

LIST OF REFERENCES

[1] Thomson, W.T., "Critical load of columns of varying cross section," J. Appl. Mech., 17 (1950), 132-134.

[2] Carslaw, H.S., and Jaeger, J.C., Conduction of Heat in Solids (2nd edition), Clarendon Press, Oxford, 1959.

[3] Yang, W.H. and Lee, E.H., "Modal analysis of Floquet waves in composite materials," J. Appl. Mech., 41 (1974), 429-433.

[4] Paramasivam, P. and Sridhar Rao, J.K., "Free vibrations of rectangular plates of abruptly varying stiffness," Int. J. Mech. Sci., 11 (1969), 885-895.

[5] Golub, G.H., Jenning, L. and Yang, W.H., "Waves in periodically structured media," J. Comp. Phys., 17 (1975), 349-357.

[6] Horgan, C.O., Lang, K.-W. and Nemat-Nasser, S., "Harmonic waves in layered composites: new bounds on eigenfrequencies," J. Appl. Mech., 45 (1978), 829-833.

[7] Horgan, C.O. and Nemat-Nasser, S., "Bounds on eigenvalues of Sturm-Liouville problems with discontinuous coefficients," J. Appl. Mth. Phys. (ZAMP), 30 (1979), 77-86.

[8] McNabb, A., Anderssen, R.S. and Lapwood, E.R., "Asymptotic behavior of the eigenvalues of a Sturm-Liouville system with discontinuous coefficients," J. Math. Anal. Appl., 54 (1976), 741-751.

[9] Anderssen, R.S. and Cleary, J.R., "Asymptotic structure in torsional free oscillations of the earth: I-overtone structure," Geophys. J. Roy. Astr. Soc., 39 (1974), 241-268.

[10] Lee, E.H., "A survey of variational methods for elastic wave propagation in composites with periodic structures," in Dynamics of Composites (E.H. Lee, ed.), ASME, New York, 1972, 122-138.

[11] Kohn, W., Krumhansl, J.A. and Lee, E.H., "Variational methods for dispersion relations and elastic properties of composites," J. Appl. Mech., 39 (1972), 327-336.

[12] Lang, K.-W., Determination of Dynamic Characteristics of Elastic Composite Structures, Ph.D. dissertation, Northwestern University, Evanston, 1978.

[13] Nemat-Nasser, S., "Harmonic waves in layered composites," J. Appl. Mech., 39 (1972), 850-852.

[14] Nemat-Nasser, S. and Fu, F.C.L., "Harmonic waves in layered composites: bounds on frequencies," J. Appl. Mech., 41 (1974) 288-290.

[15] Nemat-Nasser, S. and Minagawa, S., "Harmonic waves in layered composites: comparison among several schemes," J. Appl. Mech. 42 (1975), 699-704.

[16] Lang, K. W. and Nemat-Nasser, S., "Vibration and buckling of composite beams," J. Struct. Mech., 5 (1977), 395-419.

[17] Hodges, D.H., "Direct solution for Sturm-Liouville systems with discontinuous coefficients," AIAA Journal, 17 (1979), 349-357.

[18] Bickford, W.B., "Lower bounds to eigenvalues of piecewise continuous elastic systems," J. Appl. Mth. Phys. (ZAMP), 30 (1979), 65-75.

[19] Horgan, C.O. and Nemat-Nasser, S., "Variational methods for eigenvalues in composites," in Variational Methods in the Mechanics of Solids (S. Nemat-Nasser, ed.), Pergamon Press, New York, 1980, 52-58.

[20] Spence, J.P., Andry, A.N. and Horgan, C.O., "Lower bounds for eigenvalues of Sturm-Liouville problems with discontinuous coefficients: integral equation methods," Q. Appl. Math., to appear.

[21] Goodwin, B.E. and Boyce, W.E., "The vibrations of a random elastic string: the method of integral equations," Q. Appl. Math., 22 (1964), 261-266.

[22] Cochran, J.A., The Analysis of Linear Integral Equations, McGraw-Hill, New York, 1972.

[23] Tricomi, F.G., Integral Equations, Wiley, New York, 1957.

[24] Stakgold, I., The Boundary Value Problems of Mathematical Physics (Vols. I and II), McMillan, New York, 1967 and 1968.

[25] Shun, O.H., "Green's functions for composite media," Int. J. Engng. Sci., 16 (1978), 475-482.

[26] Baker, C.T.H., The Numerical Treatment of Integral Equations, Clarendon Press, Oxford, 1977.

[27] Sloan, I.H., "Iterated Galerkin method for eigenvalue problems," SIAM J. Numer. Anal., 13 (1976), 753-760.

[28] Wang, C., Gettrust, J.F. and Cleary, J.R., "Asymptotic overtone structure in eigenfrequencies of torsional modes of the earth: a model study," Geophys. J. Roy. Astr. Soc., 50 (1977), 289-302.

[29] Wirth, P.E. and Rodin, E.Y., "A unified theory of linear diffusion in laminated media," preprint, Washington University, St. Louis, 1979.

[30] Collatz, L., The Numerical Treatment of Differential Equations (3rd edition), Springer-Verlag, Berlin, 1960.

[31] Krein, M.G., "On certain problems on the maximum and minimum of characteristic values and on the Lyapunov zones of stability," AMS Translations, Ser. 2, 1 (1955), 163-187.

[32] Weinstein, A., "Sur la stabilité des plaques encastrées," C.R. Acad. Sci. Paris, 200 (1935), 107-109.

[33] Aronzajn, N. and Weinstein, A., "Existence, convergence and equivalence in the unified theory of plates and membranes," Proc. Nat. Acad. Sci. U.S.A., 27 (1941), 188-191.

[34] Bazley, N.W. and Fox, D.W., "Truncations in the method of intermediate problems for lower bounds to eigenvalues," J. Res. Nat. Bur. Stds., 65B (1961), 105-111.

[35] Fox, D.W. and Rheinboldt, W.C., "Computational methods for determining lower bounds for eigenvalues of operators in Hilbert space," SIAM Review, 8 (1966), 427-462.

[36] Buckens, F., "Eigenfrequencies of nonuniform beams," AIAA Journal, 1 (1963), 121-127.

[37] Janos, L., "Some inequalities concerning the characteristic frequencies of elastic continuum," Ann. Mat. Pur. Appl., 112 (1977), 273-283.

[38] Gutierrez, R.H., Laura, PA.A. and Grossi, R.O., "Transverse vibrations of plates with stepped thickness over a concentric circular region," J. Sound Vibr. 69 (1980), 285-295.

[39] Barone, A. and Gallego Juarez, J.A., "Flexural vibrating free edge plates with stepped thicknesses for generating high directional ultrasonic radiation," J. Acoust. Soc. Am., 51 (1972), 953-959.

[40] Gallego Juarez, J.A., "Axisymmetric vibrations of circular plates with stepped thickness," J. Sound Vibr., 26 (1973), 411-416.

[41] Vodicka, V., "Free vibrations of a composite circular membrane," J. Phys. Soc. Jap., 17 (1962), 698-702.

[42] De, S., "Vibrations of a composite circular membrane," Indian J. Pure Appl. Math., 3 (1972), 1150-1160.

[43] Noble, B., "Error analysis of collocation methods for solving Fredholm integral equations," in Topics in Numerical Analysis (J.J.H. Miller, ed.), Academic Press, London, 1973, 211-232.

[44] Spence, A., "Error bounds and estimates for eigenvalues of integral equations," Numer. Math., 29 (1978), 133-147.

[45] Spence, A., "On the convergence of the Nyström method for the integral equation eigenvalue problem," Numer. Math., 25 (1975), 57-66.